# Probing Bound Quark States as a Window into Strong QCD


**Ralf W. Gothe**

UNIVERSITY OF SOUTH CAROLINA


Strong QCD from Hadron Structure Experiments – VI
May 14-17, 2024, Nanjing University, China

南京大學 NANJING UNIVERSITY | 非微扰物理研究所 Institute for Nonperturbative Physics

- Why are $\gamma_v NN^*$ electrocouplings interesting? Probing bound valence quarks, baryon wave functions, the emergence of mass, and finally strong QCD.
- What we learnt and is experimentally possible? Measuring the distance-dependent bound dressed quarks structure continuously mapping the transition to pQCD.
- What is needed beyond CLAS12? Beam energy and a high acceptance (exclusive), and high-luminosity detector (beam time) with good W resolution.


This work is supported in parts by the National Science Foundation under Grant PHY 10011349.

# What we learnt experimentally?

# Nuclear Excitations and Quasi-Elastic Scattering

Paticle and Nuclei, Povh et al., MAMI B

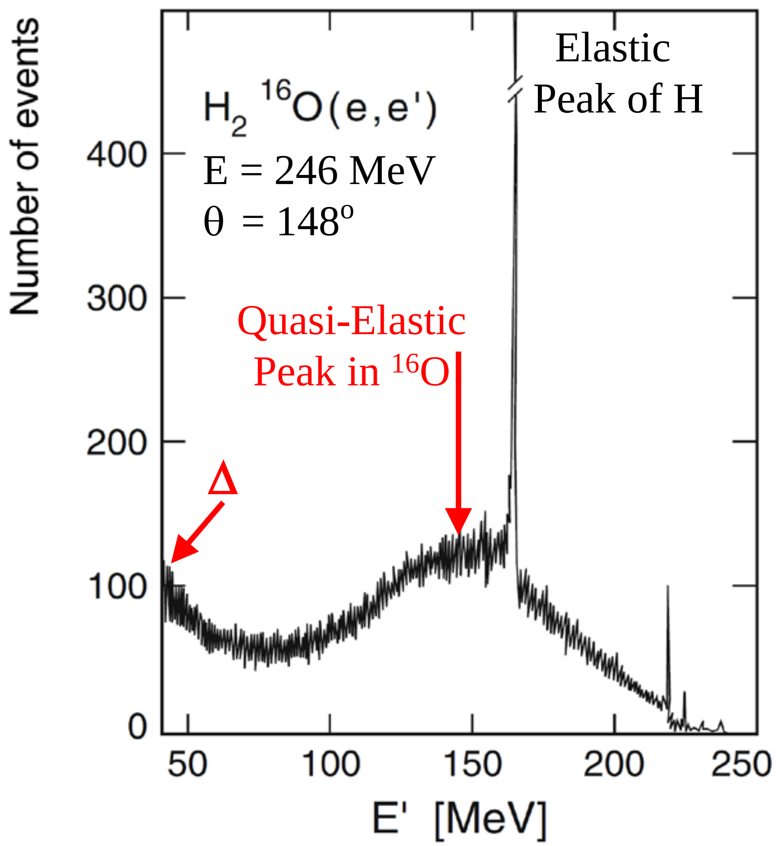


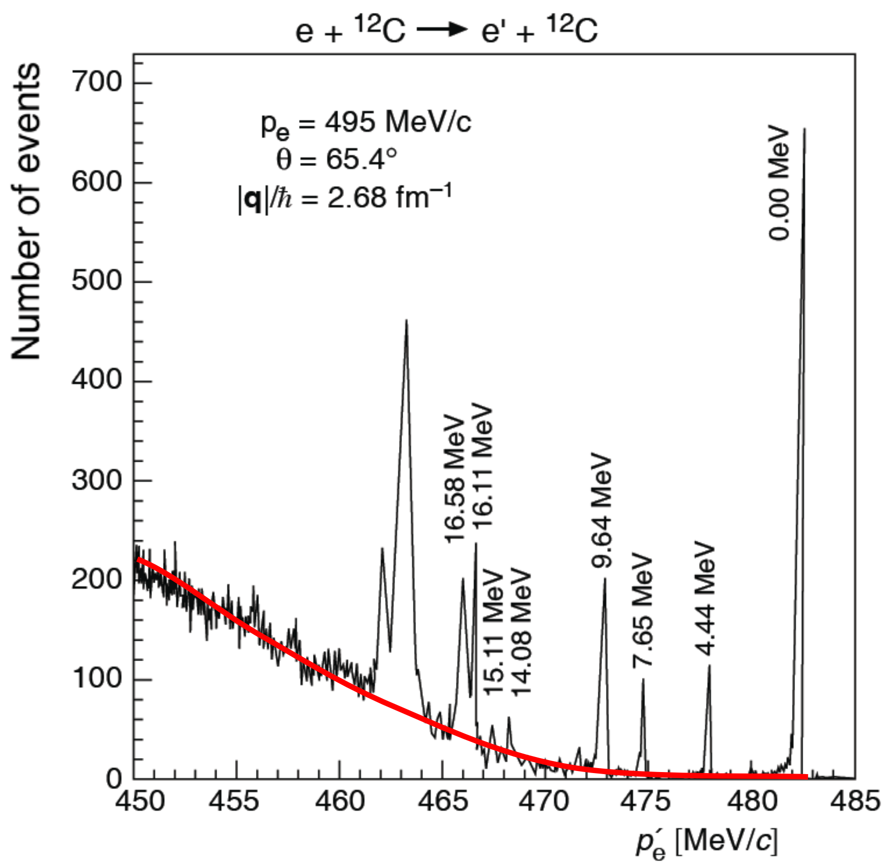


## Nucleon-Nucleus Duality

# Baryon Excitations and Quasi-Elastic Scattering

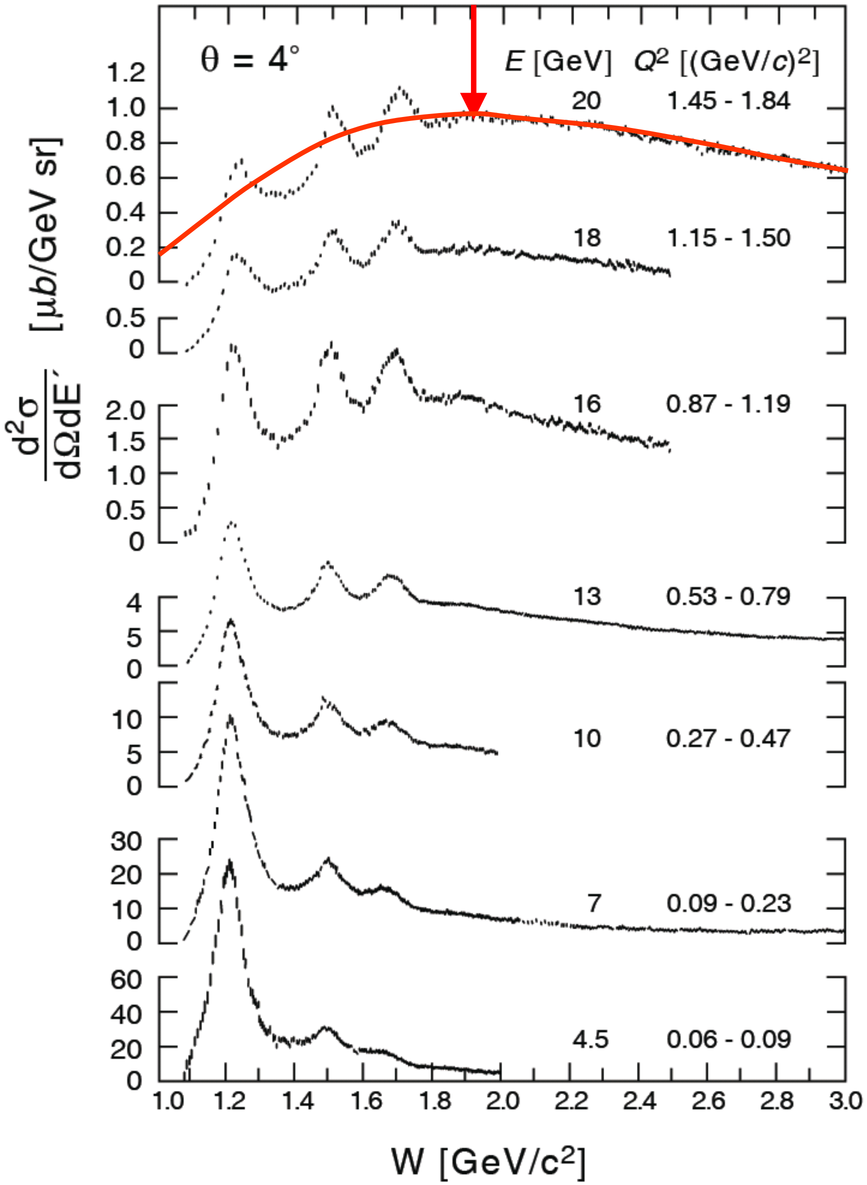


PRL **16** (1970) 1140, PR **D4** (1971) 2901
E.D. Bloom and F.J. Gilman

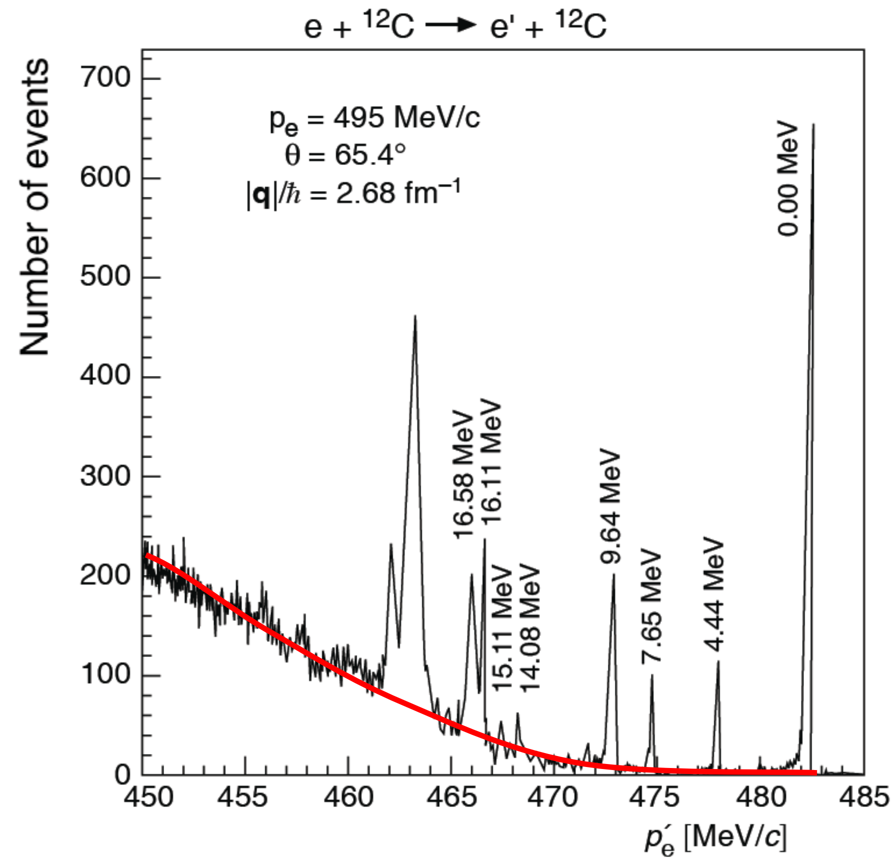


Deep Inelastic Scattering
S. Stein et al., PR **D22** (1975) 1884

# Baryon Excitations and Quasi-Elastic Scattering

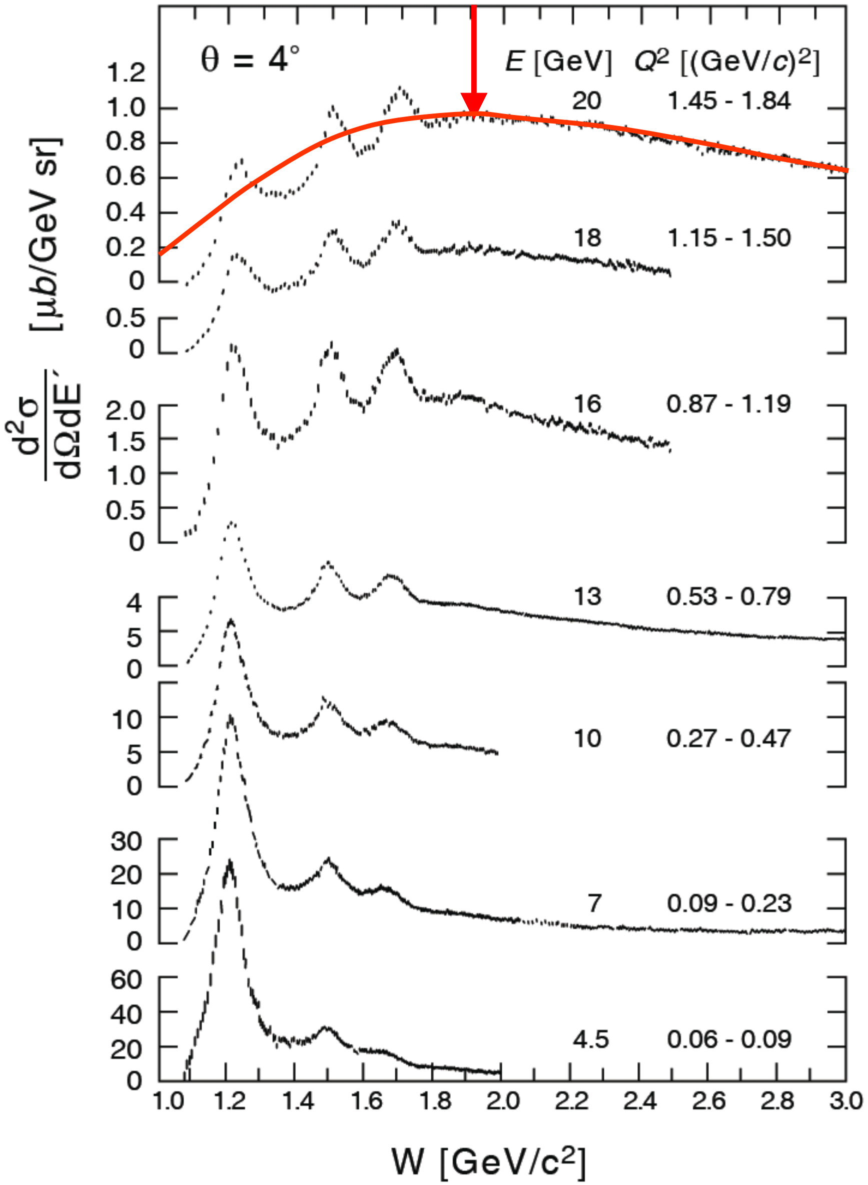


E = 20 GeV and $\theta = 4^o$

W = 1.9 GeV

E' = 17.6 GeV

$\nu = 2.37$ GeV

$Q^2 = 1.72\ GeV^2$

$m_q = 0.36$ GeV $\qquad m_q = Q^2/2\nu$

$p_F = 0.67$ GeV

$r_F = 0.79$ fm $\qquad \Delta r_F = \frac{\hbar c}{\Delta p_F} * \sqrt[3]{9\pi/2}$

Deep Inelastic Scattering
S. Stein et al., PR **D22** (1975) 1884

# Point-Like Constituents

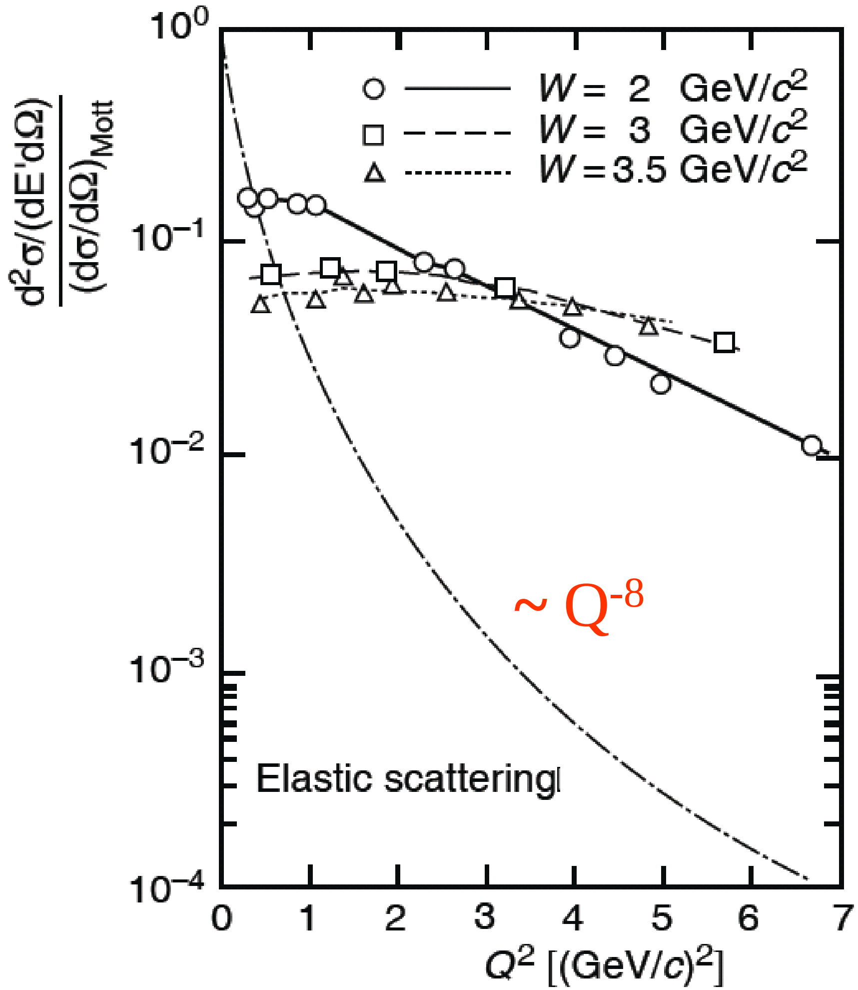


Paticle and Nuclei, Povh et al., MAMI B

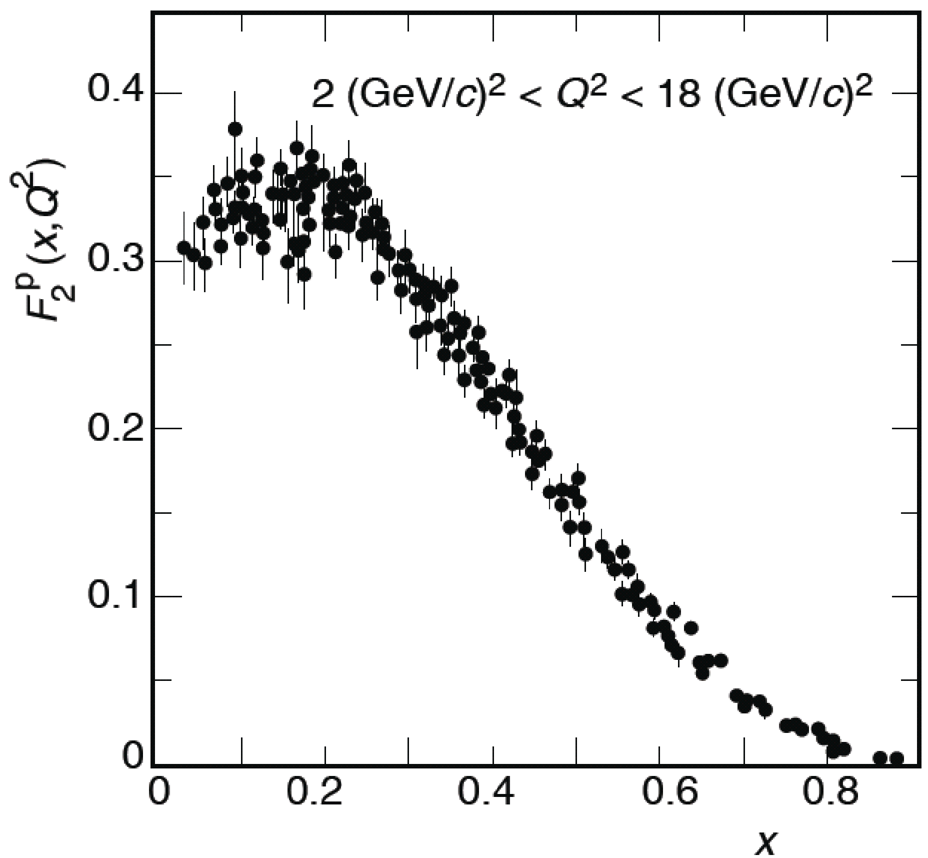


PRL **23** (1969) 935

$$\frac{d^2\sigma}{d\Omega\, dE'} = \left(\frac{d\sigma}{d\Omega}\right)_{Mott} \left[W_2(Q^2,\nu) + 2W_1(Q^2,\nu)\tan^2\frac{\theta}{2}\right]$$

# Deep-Inelastic Quasi-Eleastic Scattering

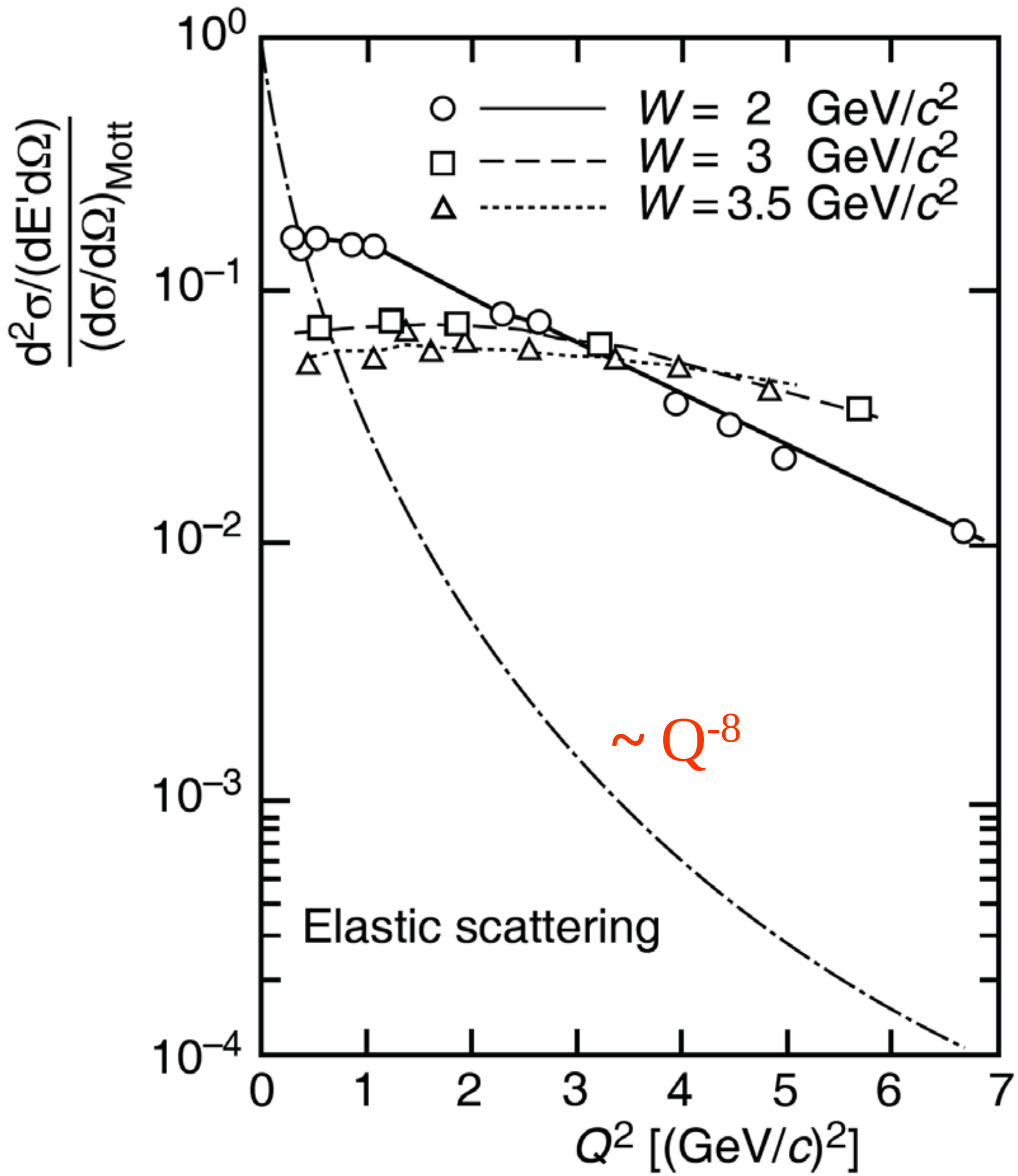


quasi-elastic off
point-like
constituents

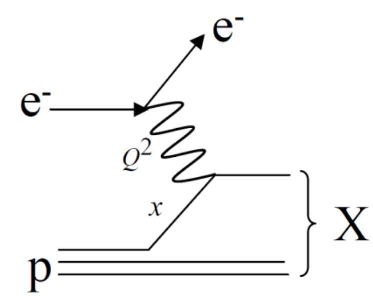


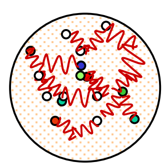

Deep Inelastic Scattering
M. Breidenbach et al.,
Phys. Rev. Lett. **23** (1969) 935

# Point-Like Constituents with Spin 1/2

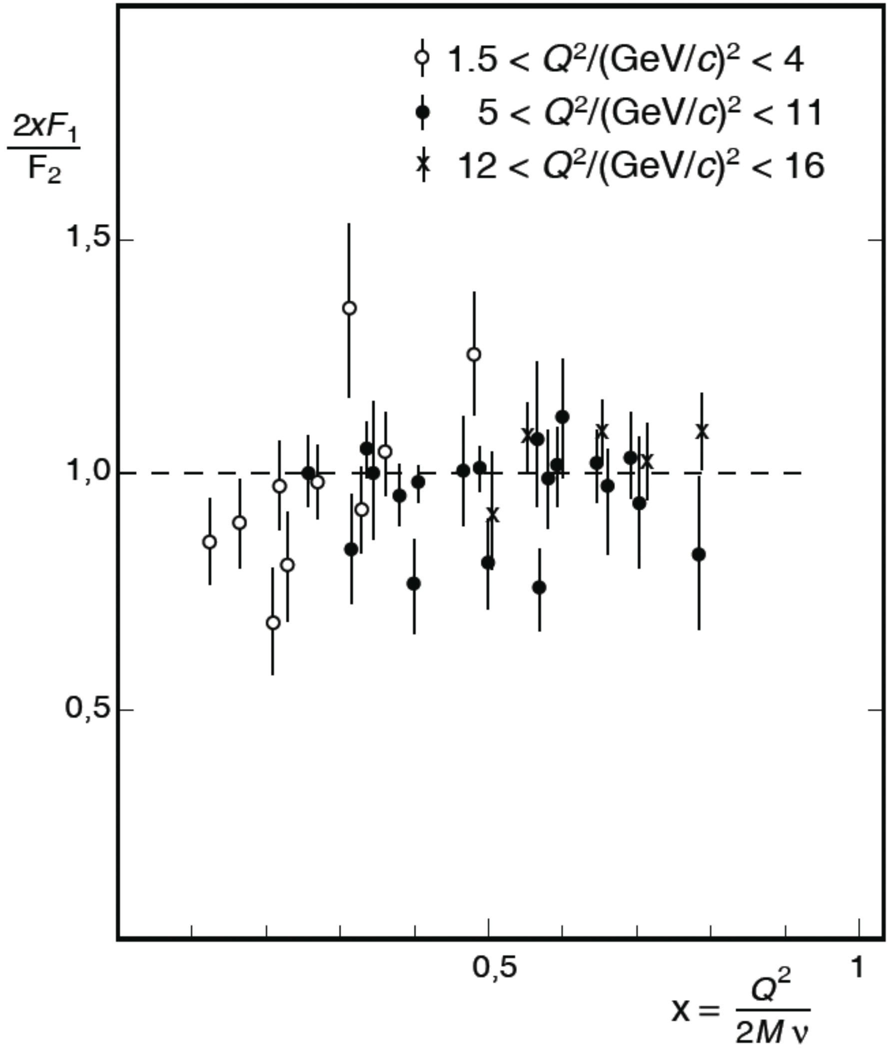


PRL **22** (1969) 156

$F_1$ structure function vanishes for spin-zero particles

Callan-Gross relation follows for spin ½ Dirac Particles

$$2xF_1(x) = F_2(x)$$

# Why is it Interesting?

# Emergence of Hadron Mass Traced by Electromagnetic Probes

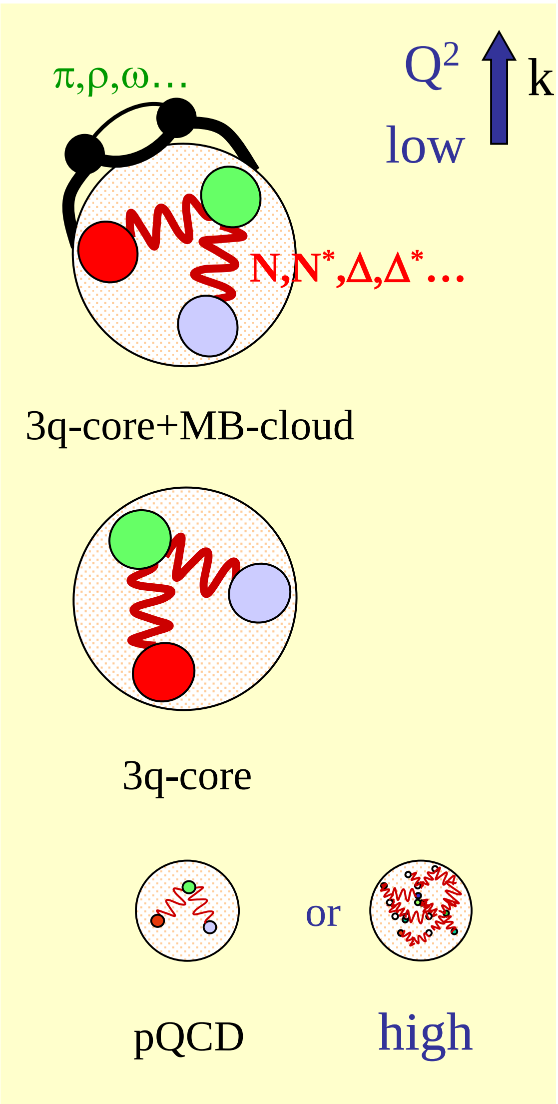


SM

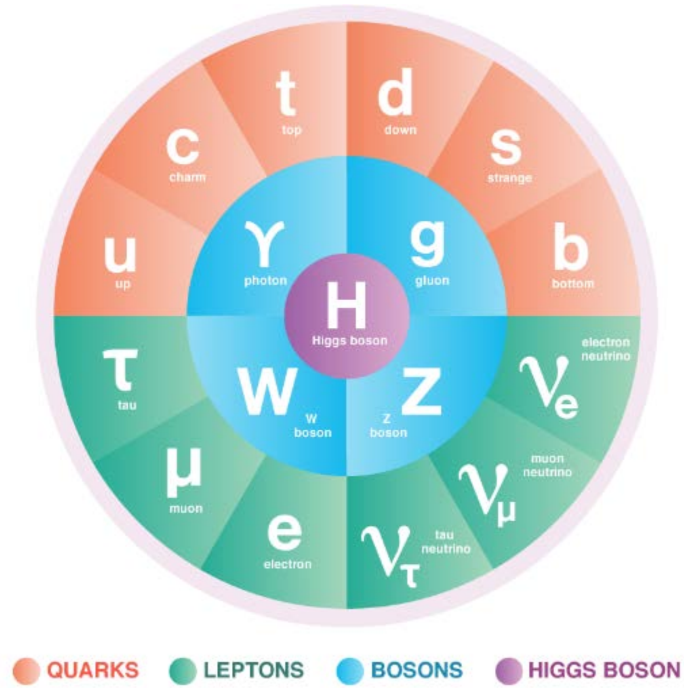


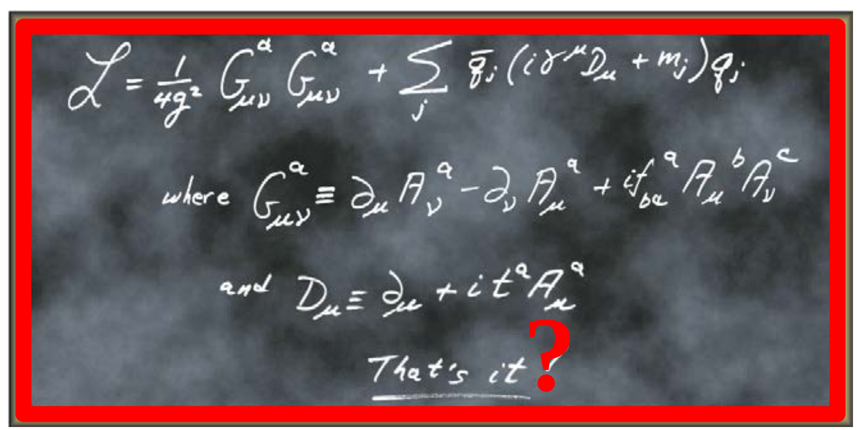


Frank Wilczek, Physics Today, August 2000

# Hadron Structure with Electromagnetic Probes

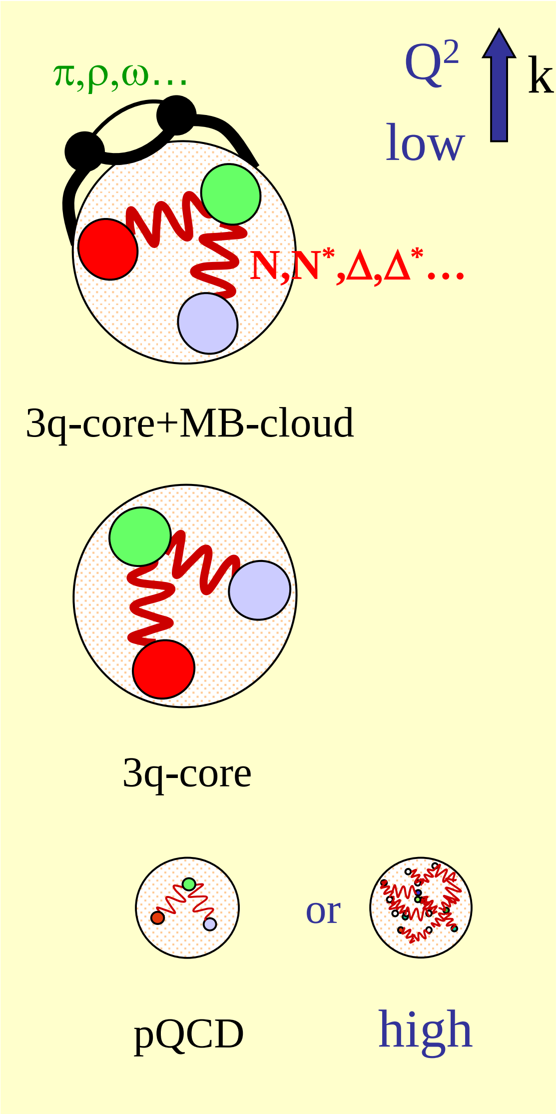


- The SM $\alpha_s$ diverges as $\Lambda_{QCD}^2$ approaches zero, but confinement and the meson cloud heal this artificial divergence as QCD becomes non-perturbative.

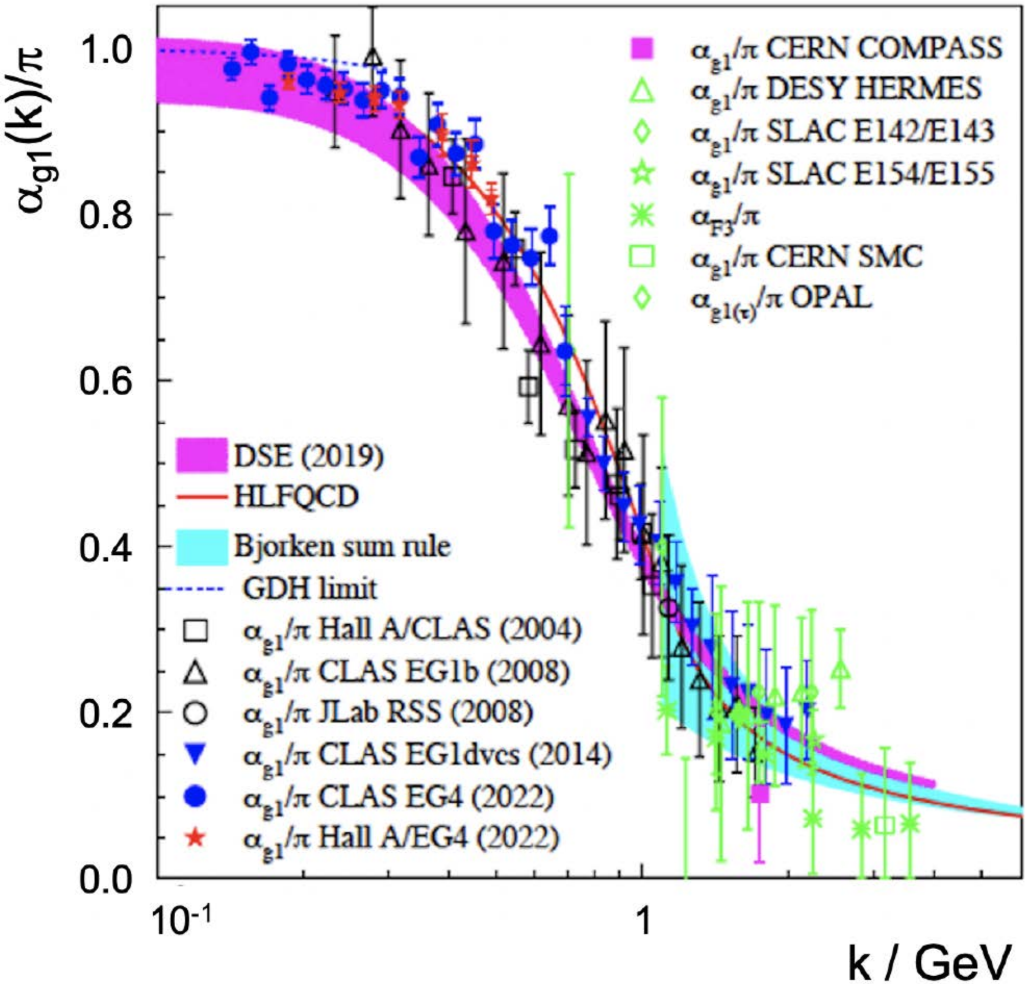

# Experimental Approach to Hadron Mass

# Hadron Structure with Electromagnetic Probes

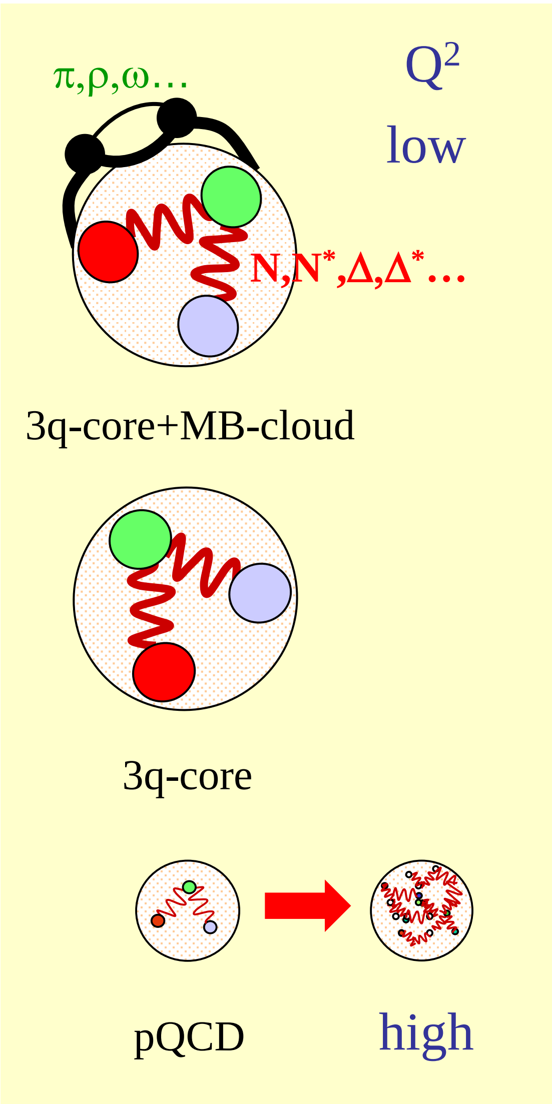


- Scaling violation in quasi-elastic lepton scattering of point-like quarks.

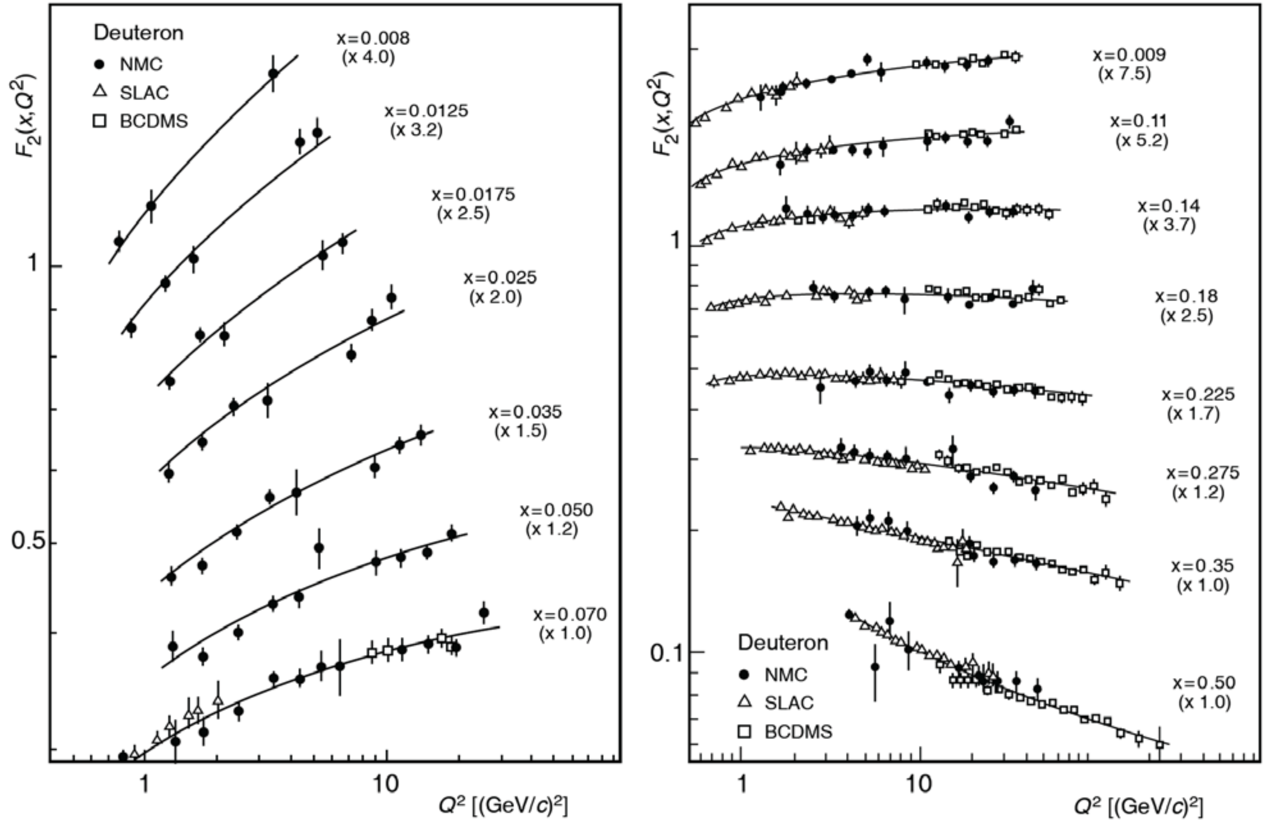


$$\Rightarrow \quad F_2(x) = x \cdot \sum_f z_f^2 \left( q_f(x) + \bar{q}_f(x) \right)$$

# Deep Inelastic Scattering

$$W^2c^2 = P'^2 = (P + q)^2 = M^2c^2 + 2Pq + q^2 = M^2c^2 + 2M\nu - Q^2 = M^2c^2$$

## Elastic

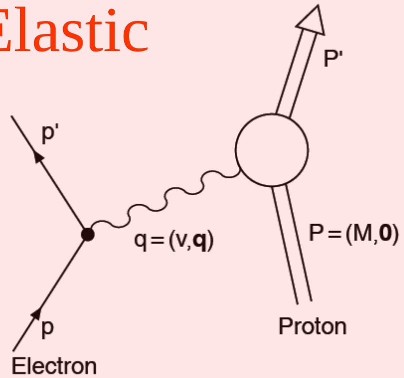


$$W = M \quad 2M\nu - Q^2 = 0$$

$$x = 1$$

$$x := \frac{Q^2}{2Pq} = \frac{Q^2}{2M\nu}$$

## DIS

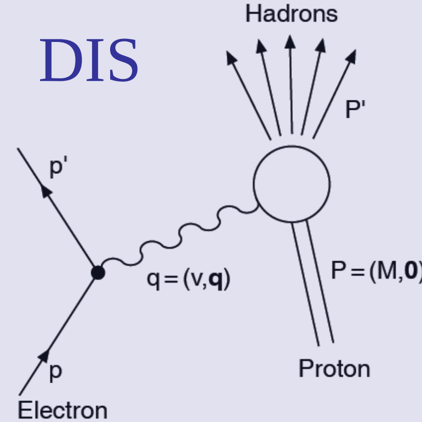


$$W > M \quad 2M\nu - Q^2 > 0$$

$$0 < x < 1$$

$$W^2c^2 = P'^2 = (P + q)^2 = m^2c^2 + 2Pq + q^2 = m^2c^2 + 2m\nu - Q^2 = m^2c^2$$

## Quasi-Elastic

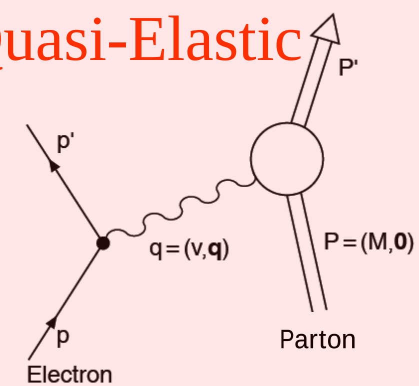


$$x = \frac{Q^2}{2M\nu} = \frac{m}{M} \quad \text{since} \quad 1 = \frac{Q^2}{2m\nu}$$

# Hadron Structure and Emergence of Hadron Mass

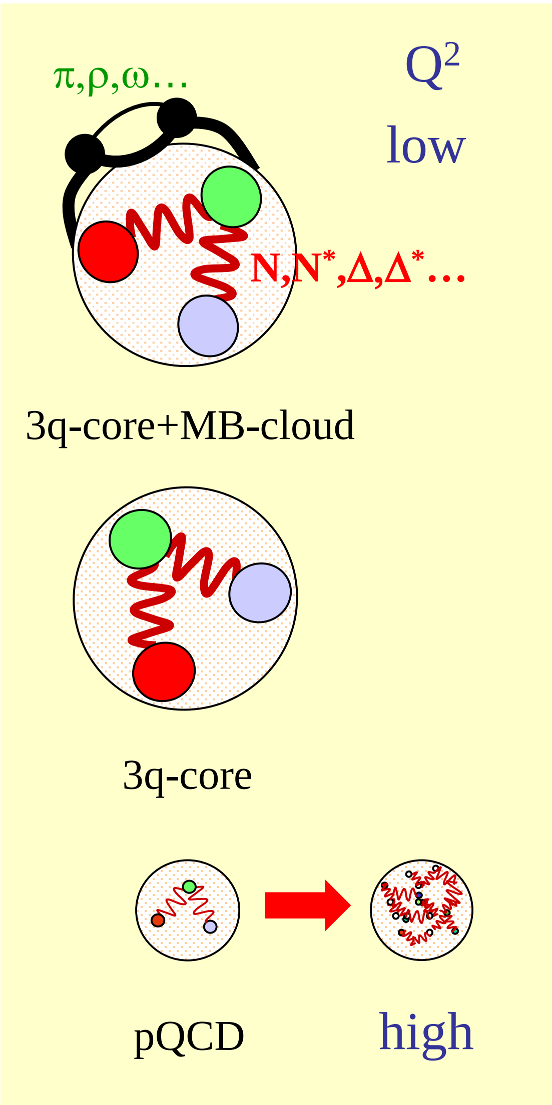


- Study the structure of the nucleon ground state.

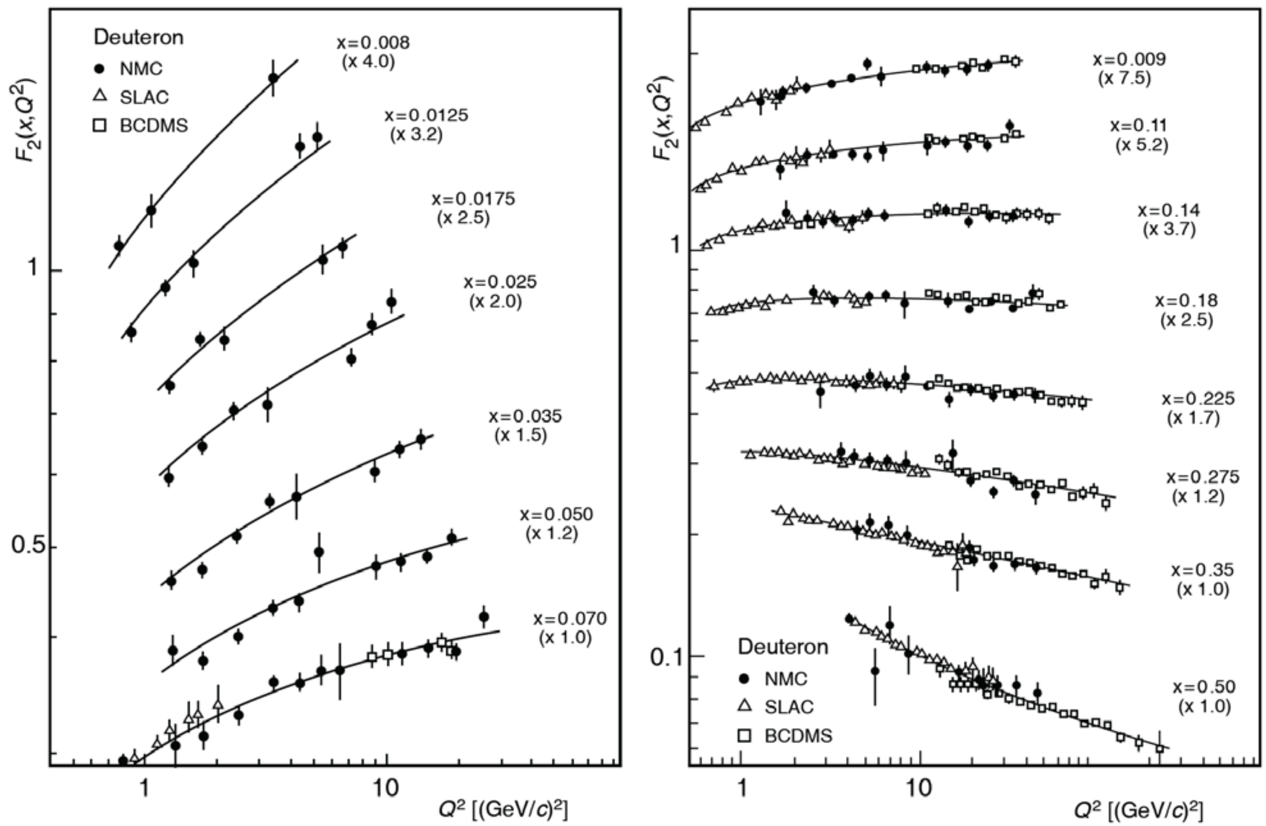


$$F_2(x) = x \cdot \sum_f z_f^2 \left(q_f(x) + \bar{q}_f(x)\right)$$

# Hadron Structure with Electromagnetic Probes

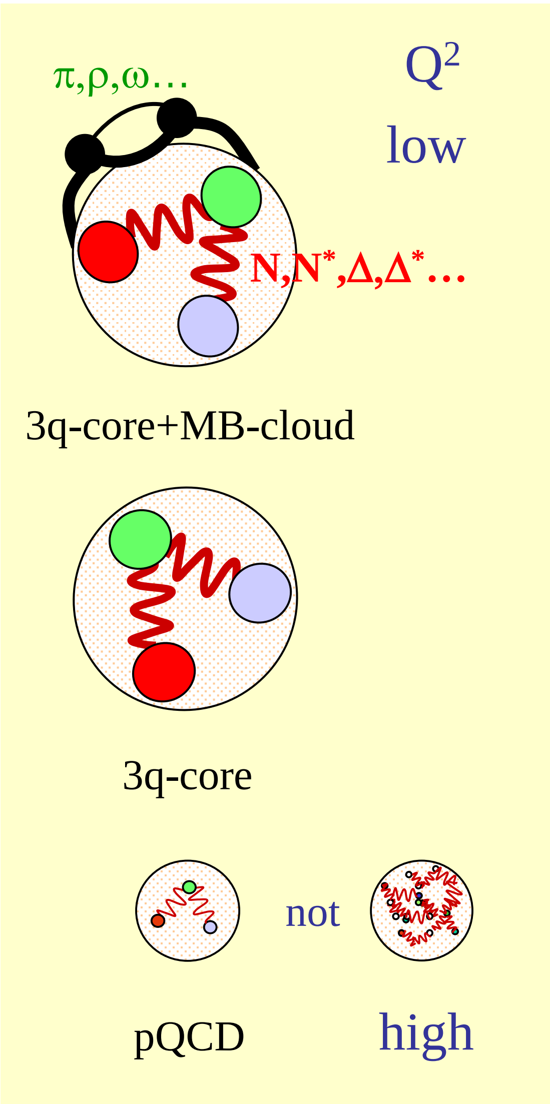


- Study the three bound quark structure of baryons in the domain where most of the mass is generated by the strong field and continuously probe it towards pQCD.

quasi-elastic

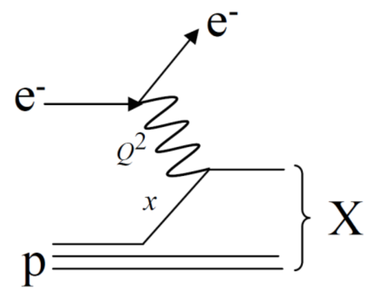


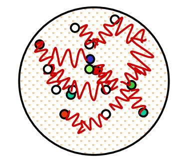

hard and bound

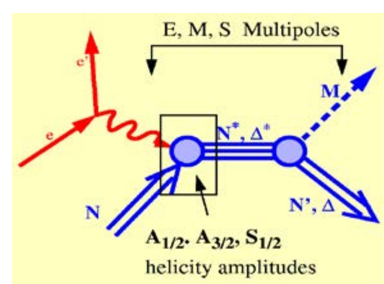


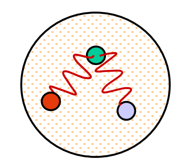

# Emergence of Hadron Mass Traced by Electromagnetic Probes

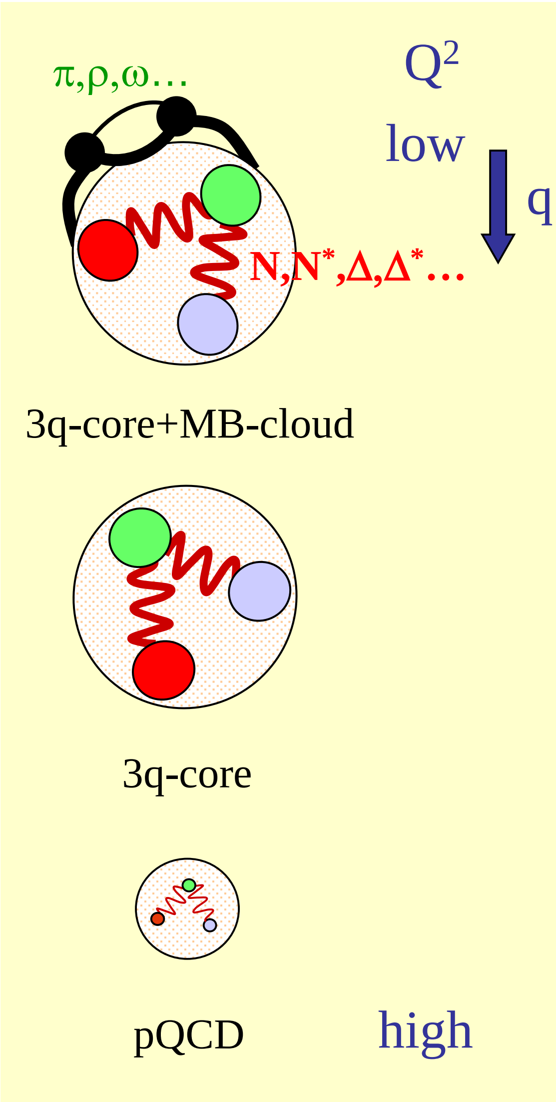


- Study the structure of the nucleon spectrum in the domain where dressed quarks are the major active degree of freedom.

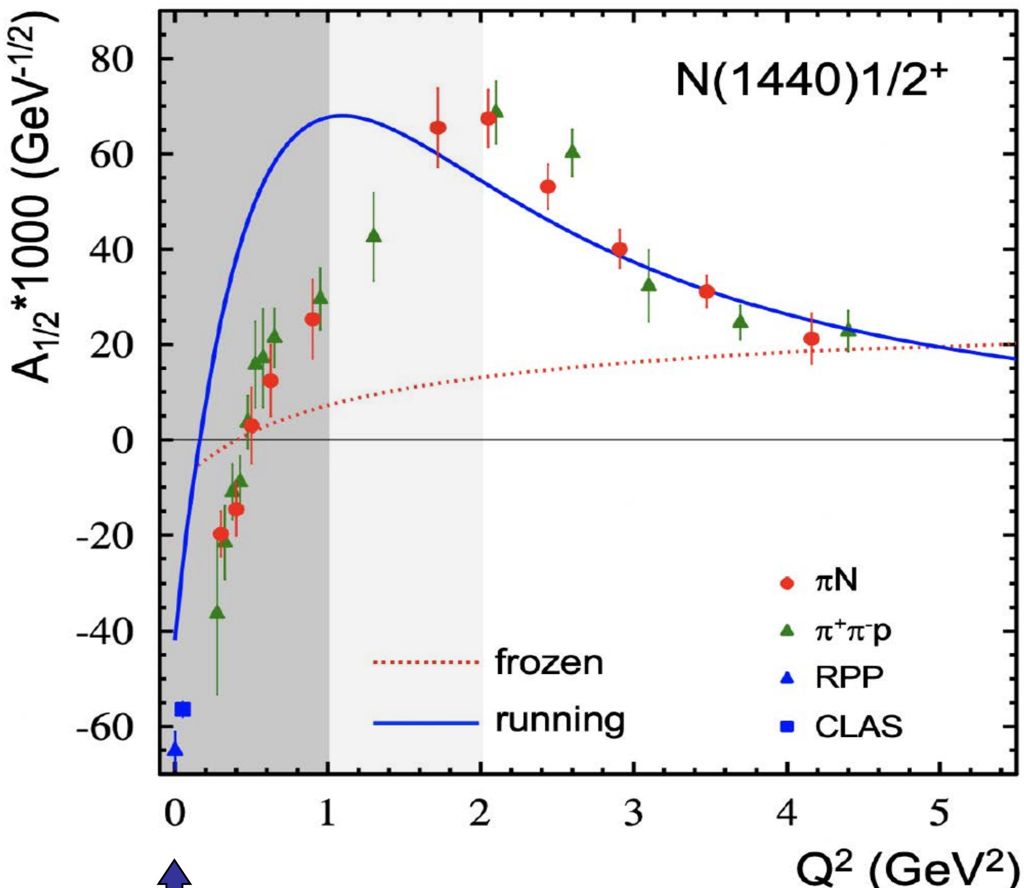


e.m. probe

# Emergence of Hadron Mass Traced by Electromagnetic Probes

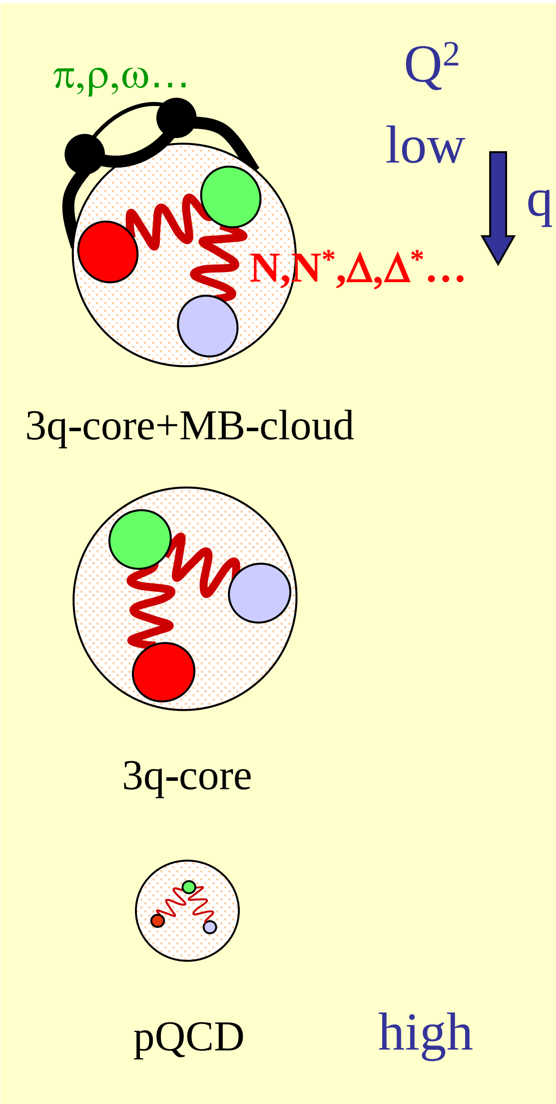


- Study the structure of the nucleon spectrum in the domain where most of the mass is generated by the strong field and dressed quarks are the major active degree of freedom.

Zhu-Fang Cui et al., Chin. Phys. C **44** (2020) 083102/1-10

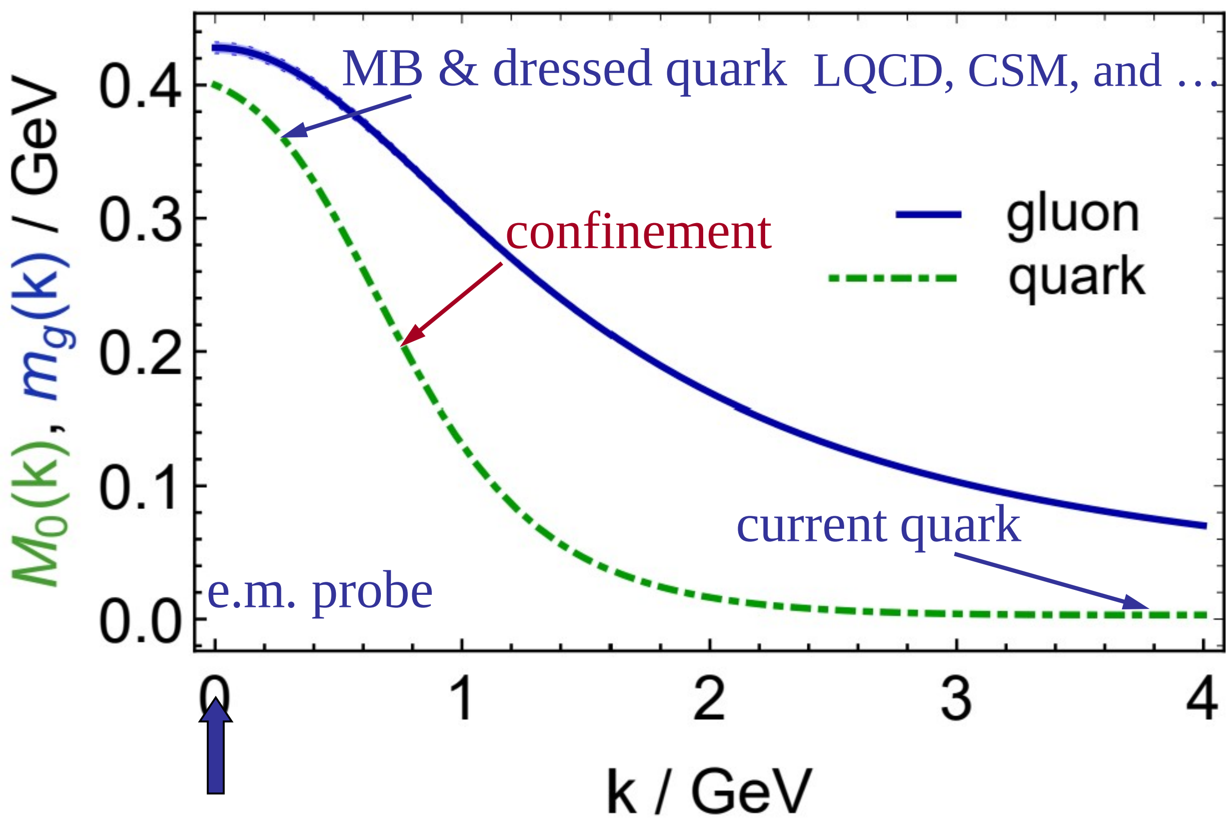

# CLAS

# Data-Driven Data Analyses

## Consistent Results

Single Pion

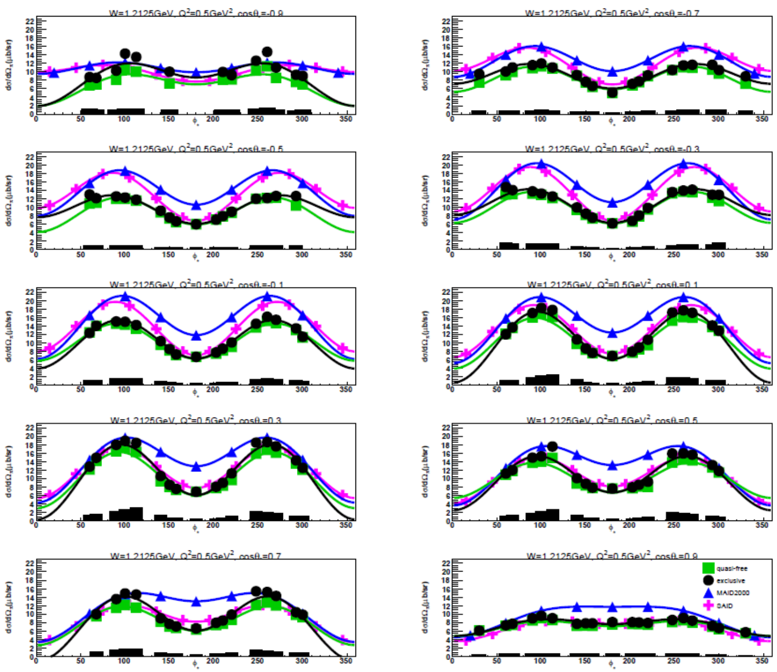

Int. J. Mod. Phys. E, Vol. 22, 1330015 (2013) 1-99

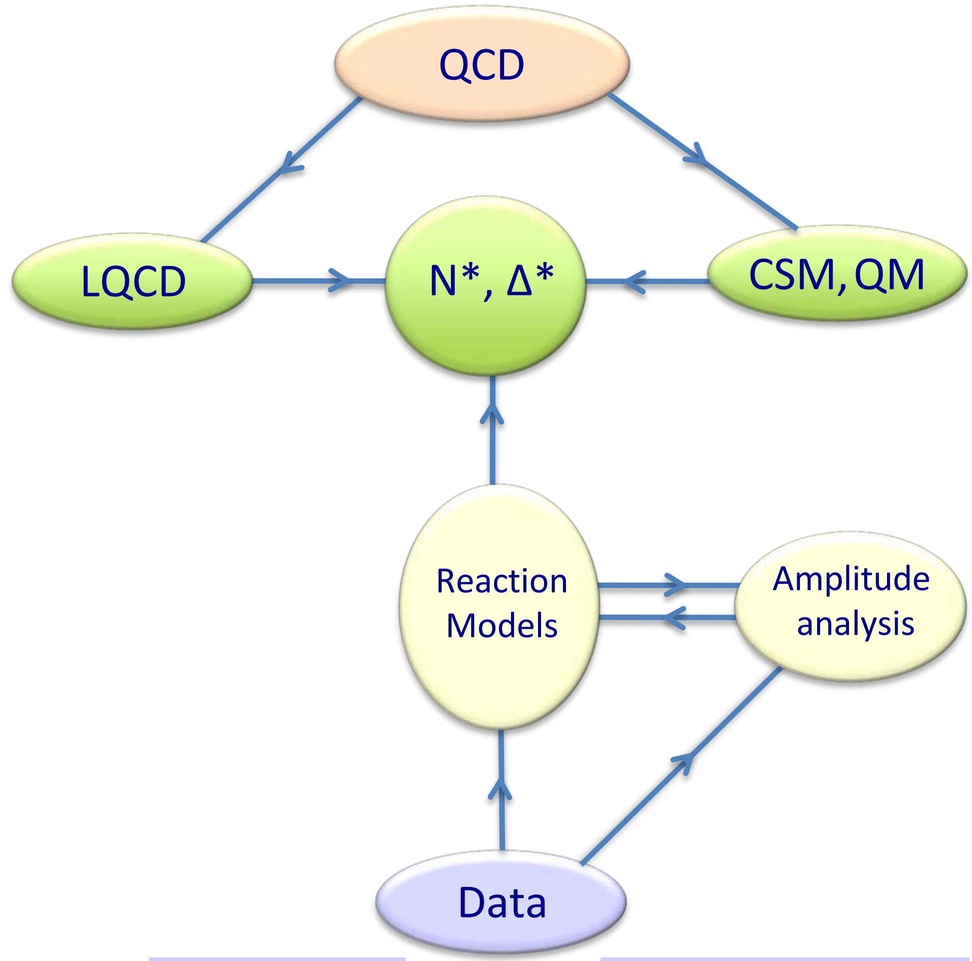


Hadronic production

Electromagnetic production

# Exclusive Single $\pi^-$ Electroproduction off the Deuteron

Y. Tian *et al.*, Phys. Rev. **C 107**, 015201 (2023) 26

W = 1.2125 GeV

ΔW = 25 MeV

$Q^2 = 0.5\ GeV^2$

$\Delta Q^2 = 0.2\ GeV^2$

cos(θ) = -0.7
Δcos(θ) = 0.2
cos(θ) = 0.9

ϕ = 20°
Δϕ = 40°
ϕ = 340°

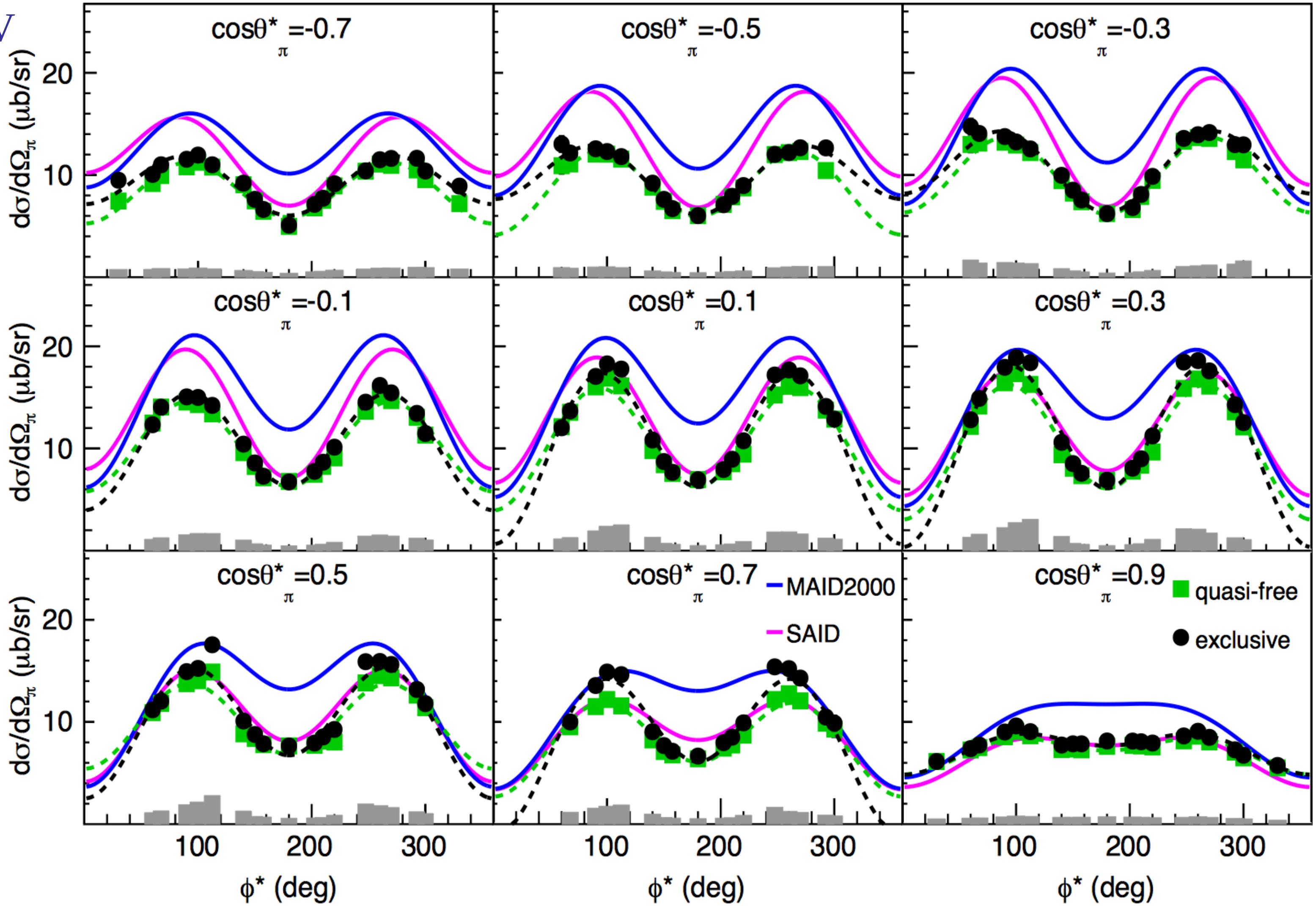

# Exclusive Single $\pi^-$ Electroproduction off the Deuteron

Ye Tian

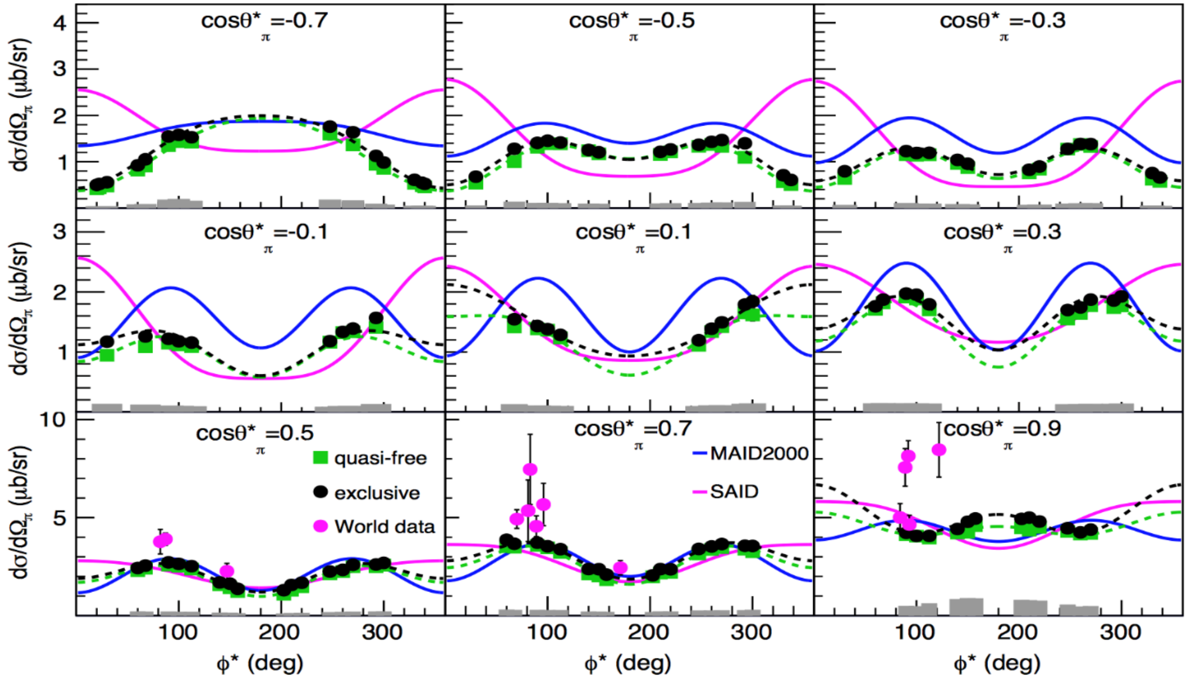


W = 1.5125 GeV

$Q^2 = 0.5\ \mathrm{GeV}^2$

$\Delta Q^2 = 0.2\ \mathrm{GeV}^2$

W = 1.6625 GeV

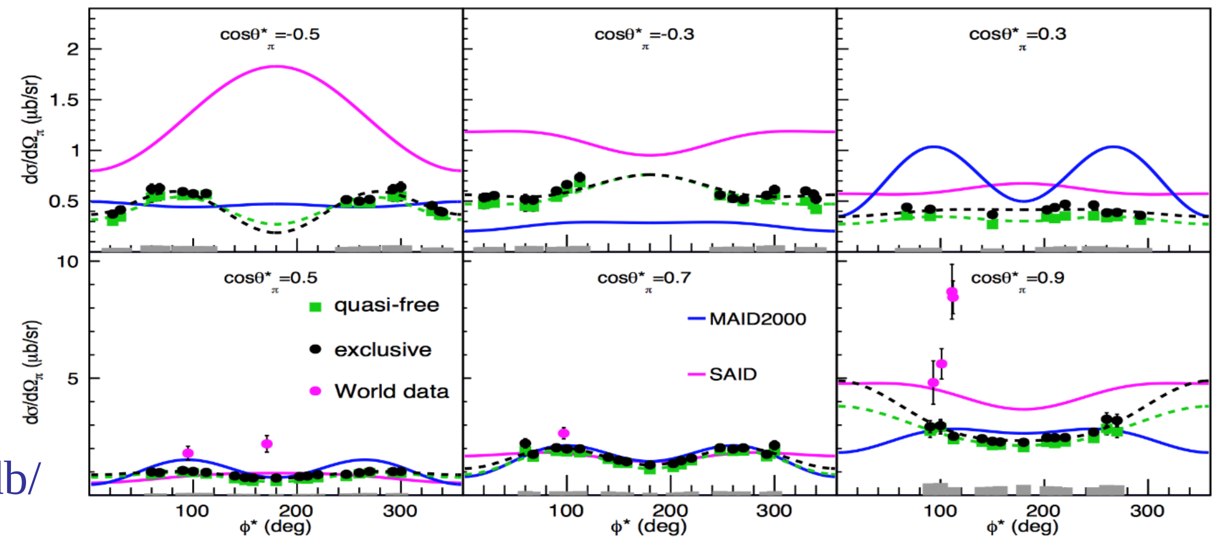


CLAS Database:
https://clasweb.jlab.org/physicsdb/

# cos $\theta_\pi$- Dependent Structure Functions @ W=1.2125 GeV

W = 1.2125 GeV ΔW = 25 MeV Ye Tian

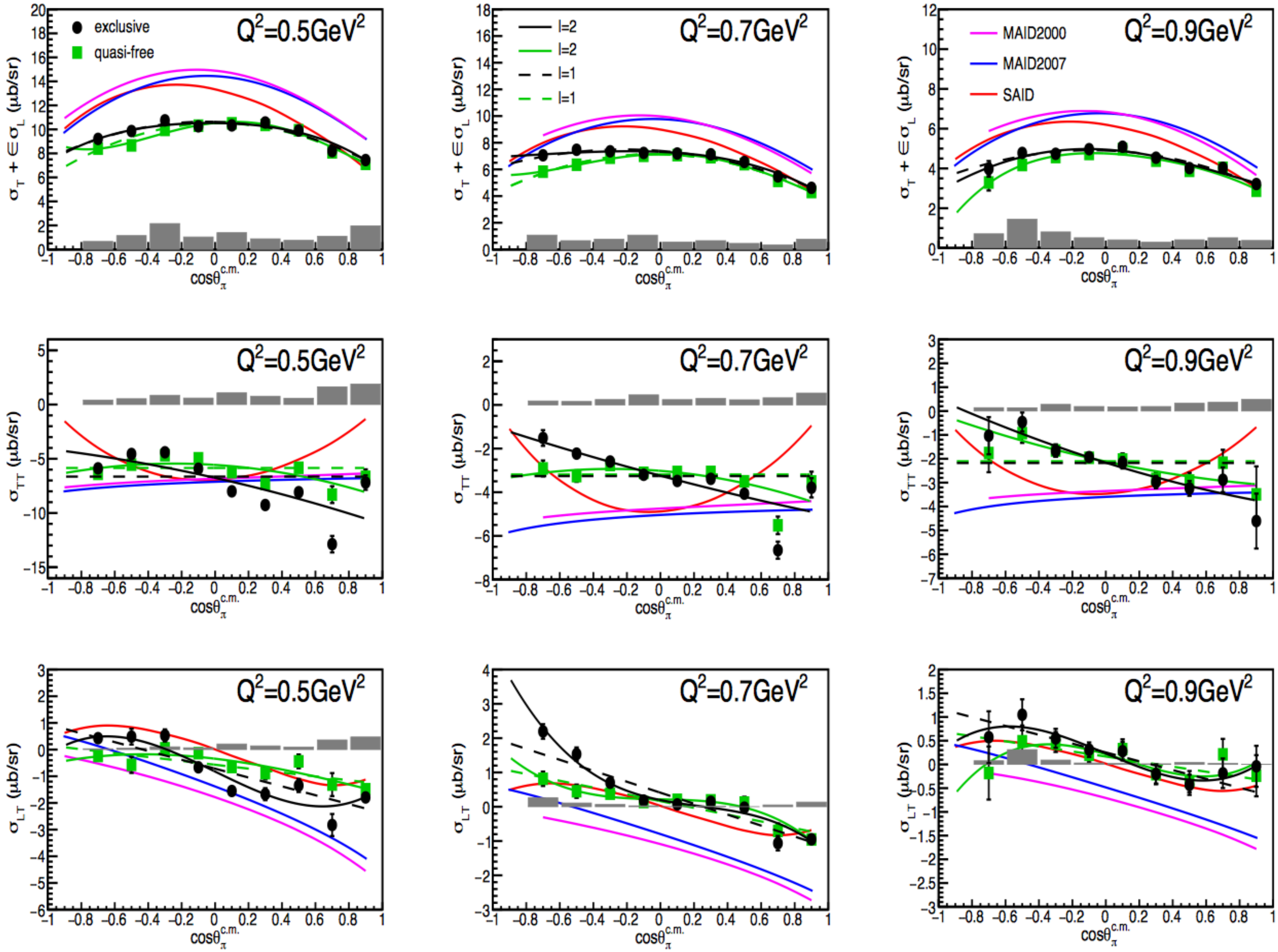

# Roper Transition Form Factors in CSM Approach

**$N(1440)P_{11}$**

J. Segovia *et al.*, Phys. Rev. Lett. 115, 171801 (2015)

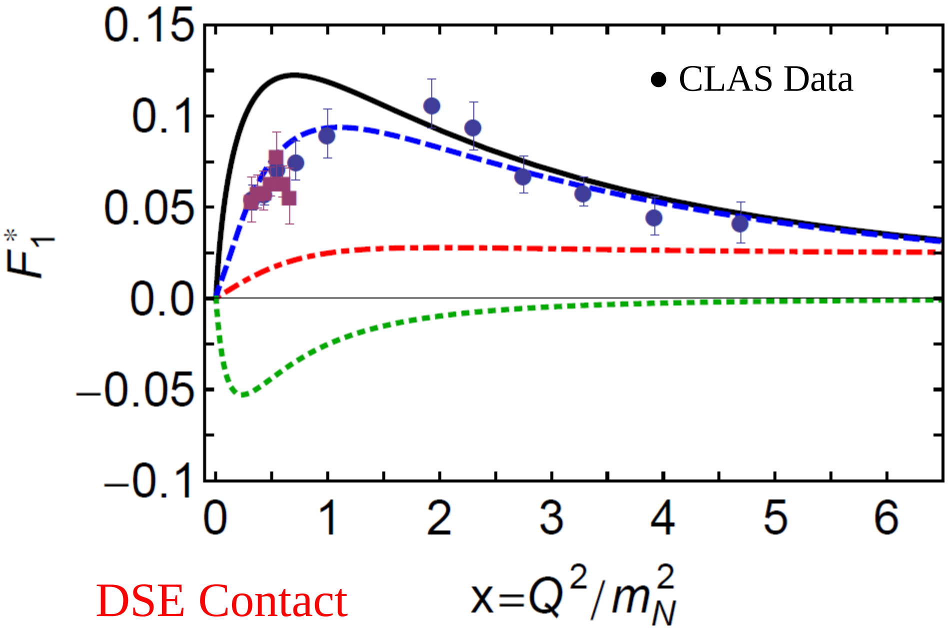


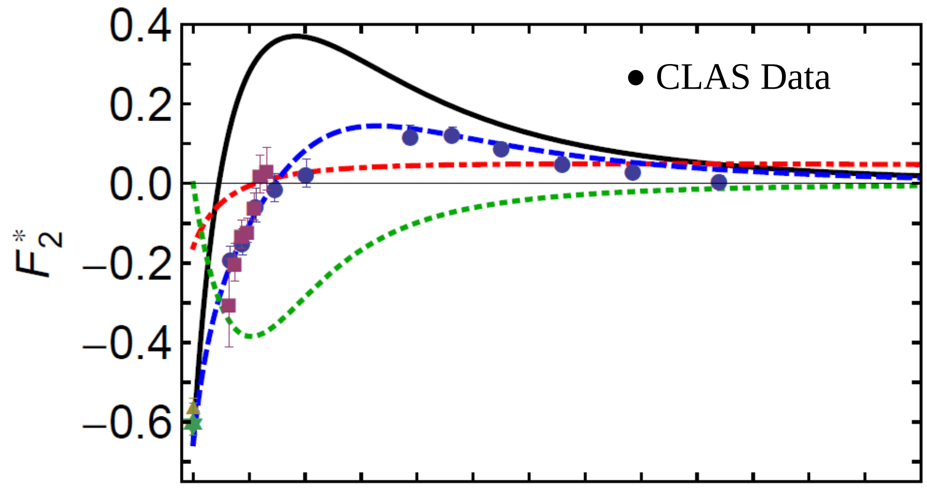


DSE Contact

DSE Realistic

Inferred meson-cloud contribution

Anticipated complete result

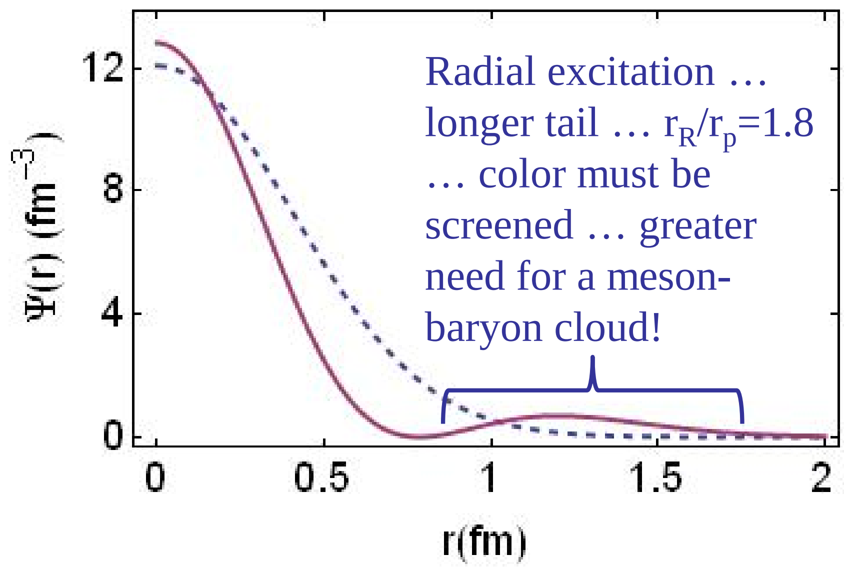


Importantly, the existence of a zero in $F_2$ is not influenced by meson-cloud effects, although its precise location is.

# Roper Transition Form Factors in CSM Approach

Y. Tian *et al.*, Phys. Rev. **C 107**, 015201 (2023) 26

$N(1440)P_{11}$

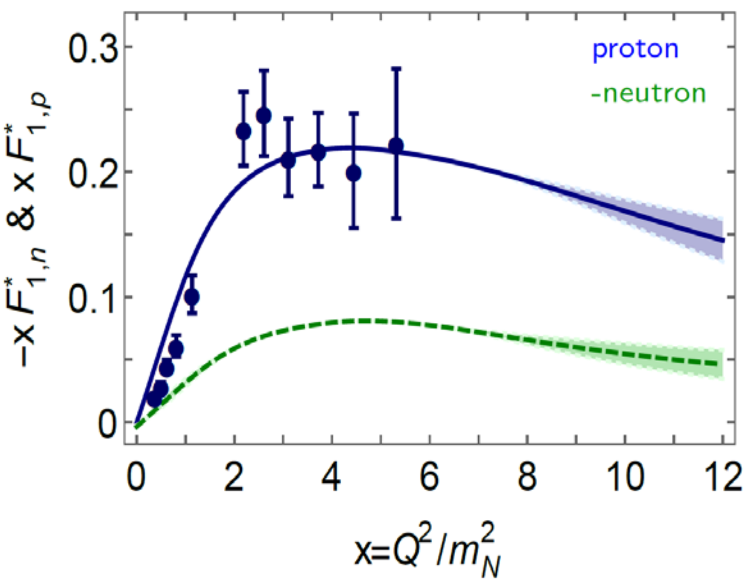


W = 1.2125 GeV

W = 1.5125 GeV

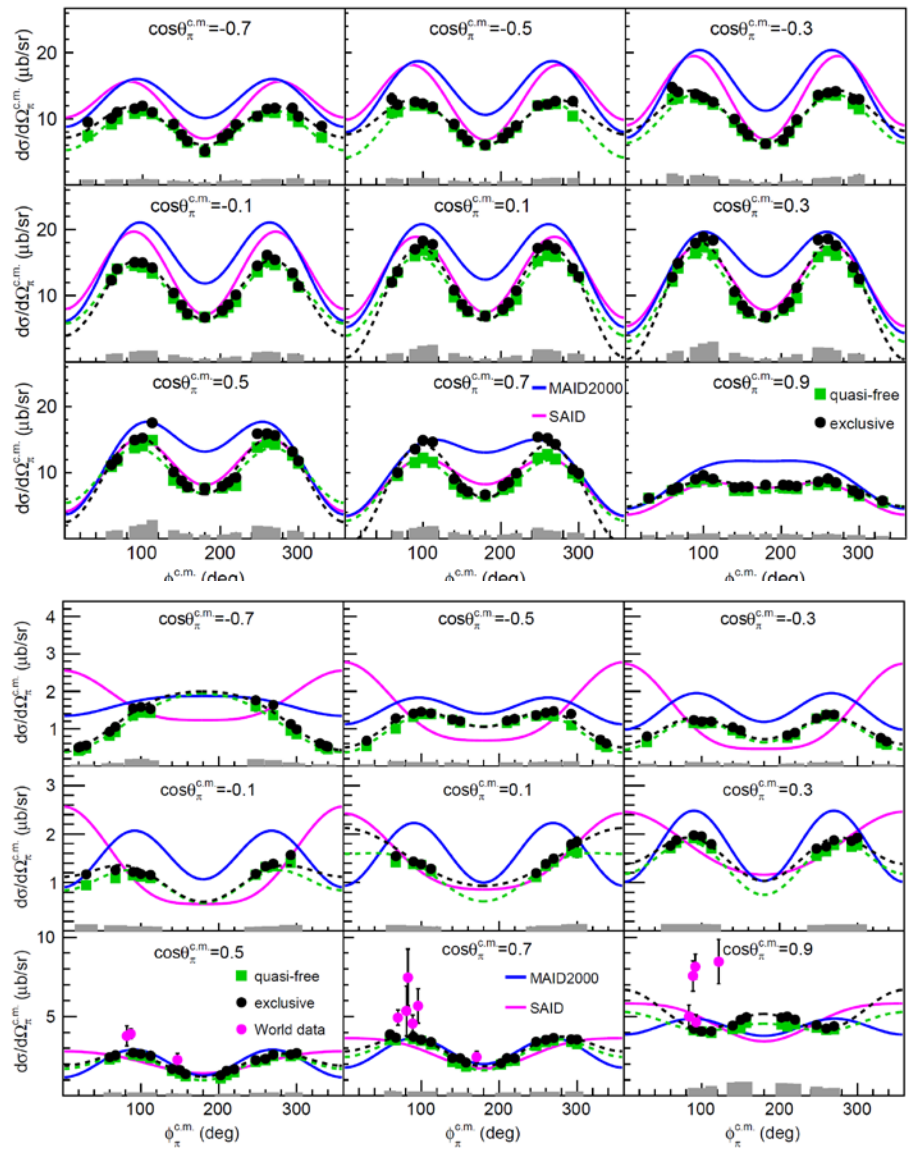

# Data-Driven Data Analyses

## Consistent Results

Double Pion

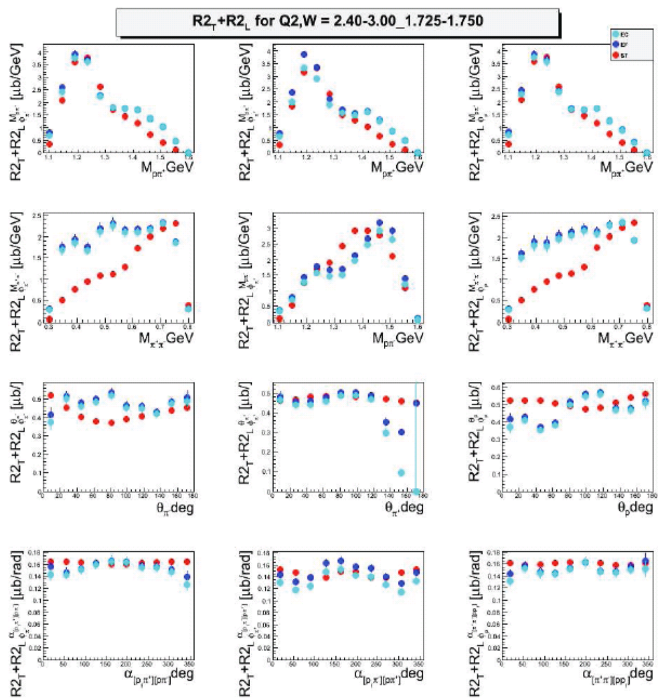


Int. J. Mod. Phys. E, Vol. 22, 1330015 (2013) 1-99

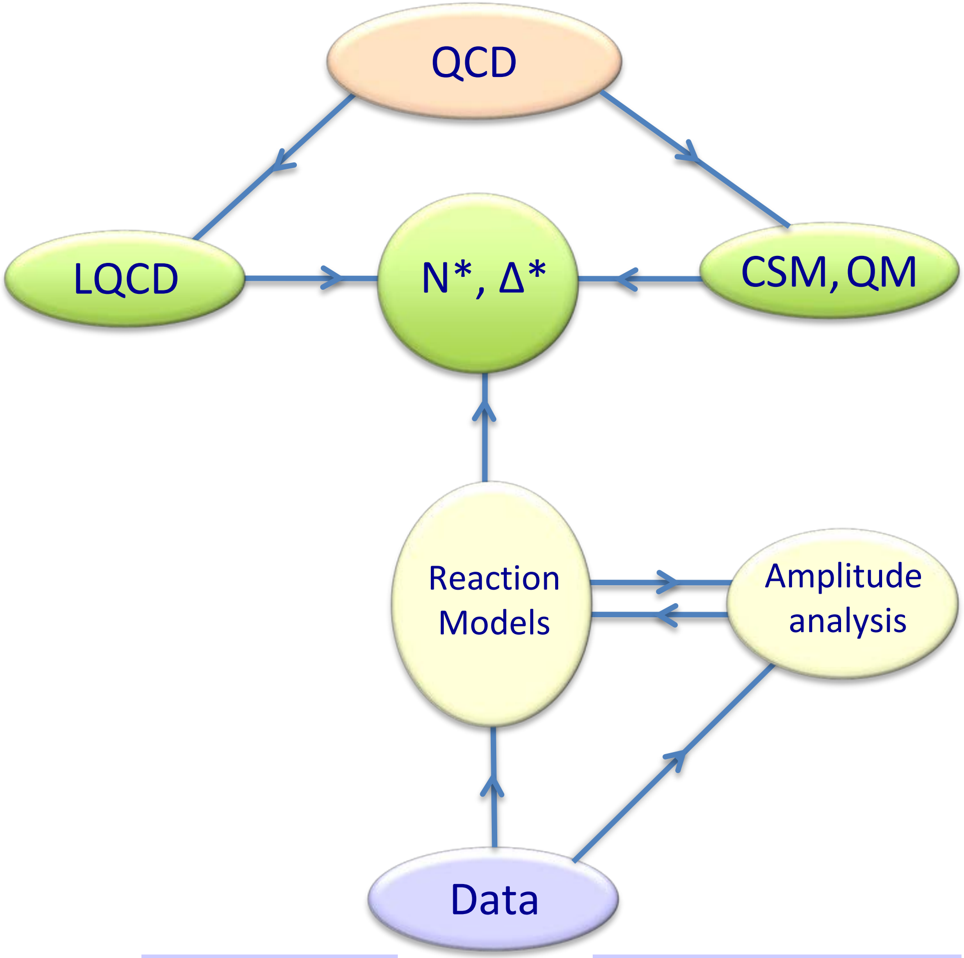


Hadronic production

Electromagnetic production

# φ-independent Nππ Single-Differential Cross Sections

$Q^2, W \text{ bin} = [2.4, 3.0) GeV^2, [1.725, 1.750) GeV$

Arjun Trivedi
Evgeny Isupov

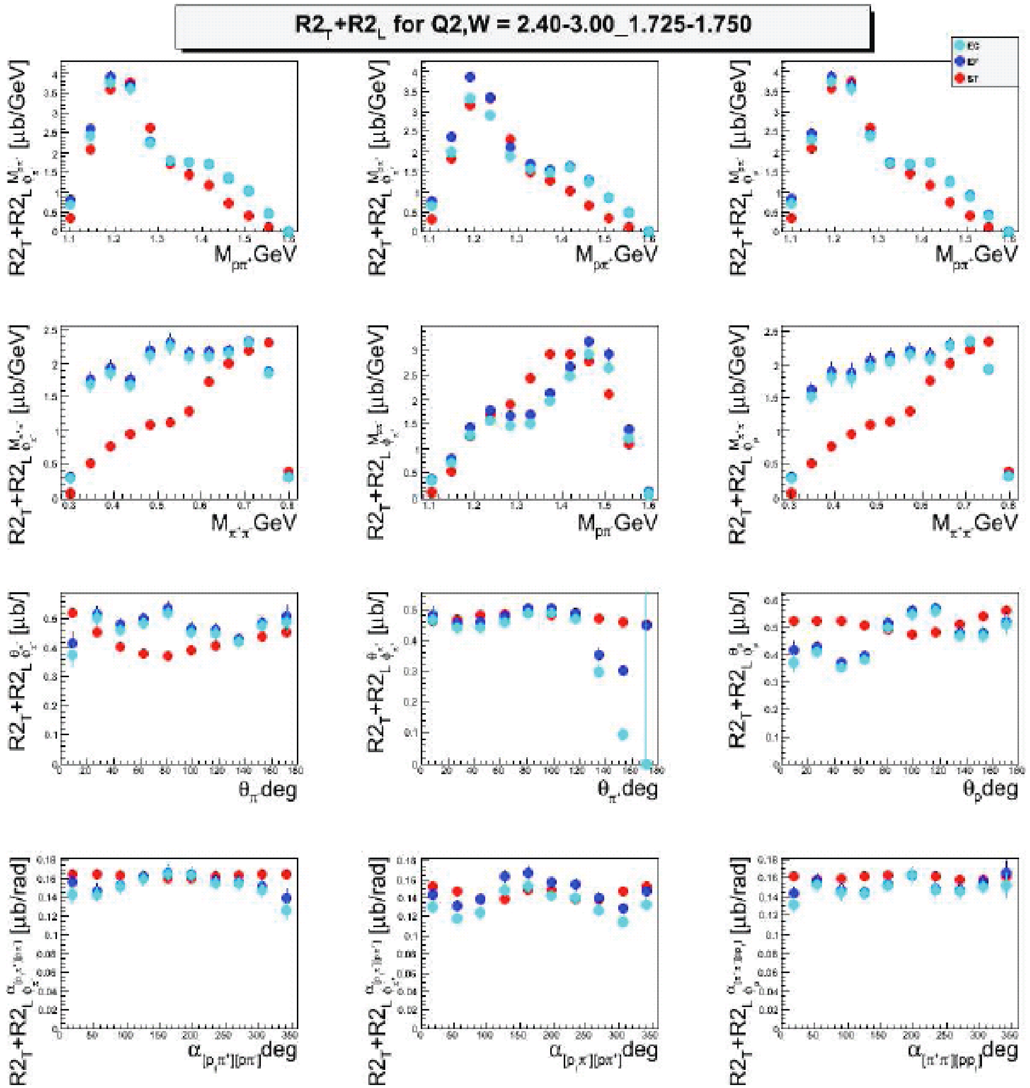


- normalized
- hole filled
- TWOPEG

$$\left(\frac{d^2\sigma}{dX_{ij}d\phi_i}\right) = \underline{R2_T{}^{X_{ij}} + R2_L{}^{X_{ij}}} + R2_{LT}{}^{c,X_{ij}}\cos\phi_i + R2_{TT}{}^{c,X_{ij}}\cos 2\phi_i + \delta_{X_{ij}\alpha_i}\left(R2_{LT}{}^{s,\alpha_i}\sin\phi_i + R2_{TT}{}^{s,\alpha_i}\sin 2\phi_i\right)$$

# φ-dependent Nππ Single-Differential Cross Sections

$Q^2, W$ bin $= [2.4, 3.0)GeV^2, [1.725, 1.750)GeV$

Arjun Trivedi

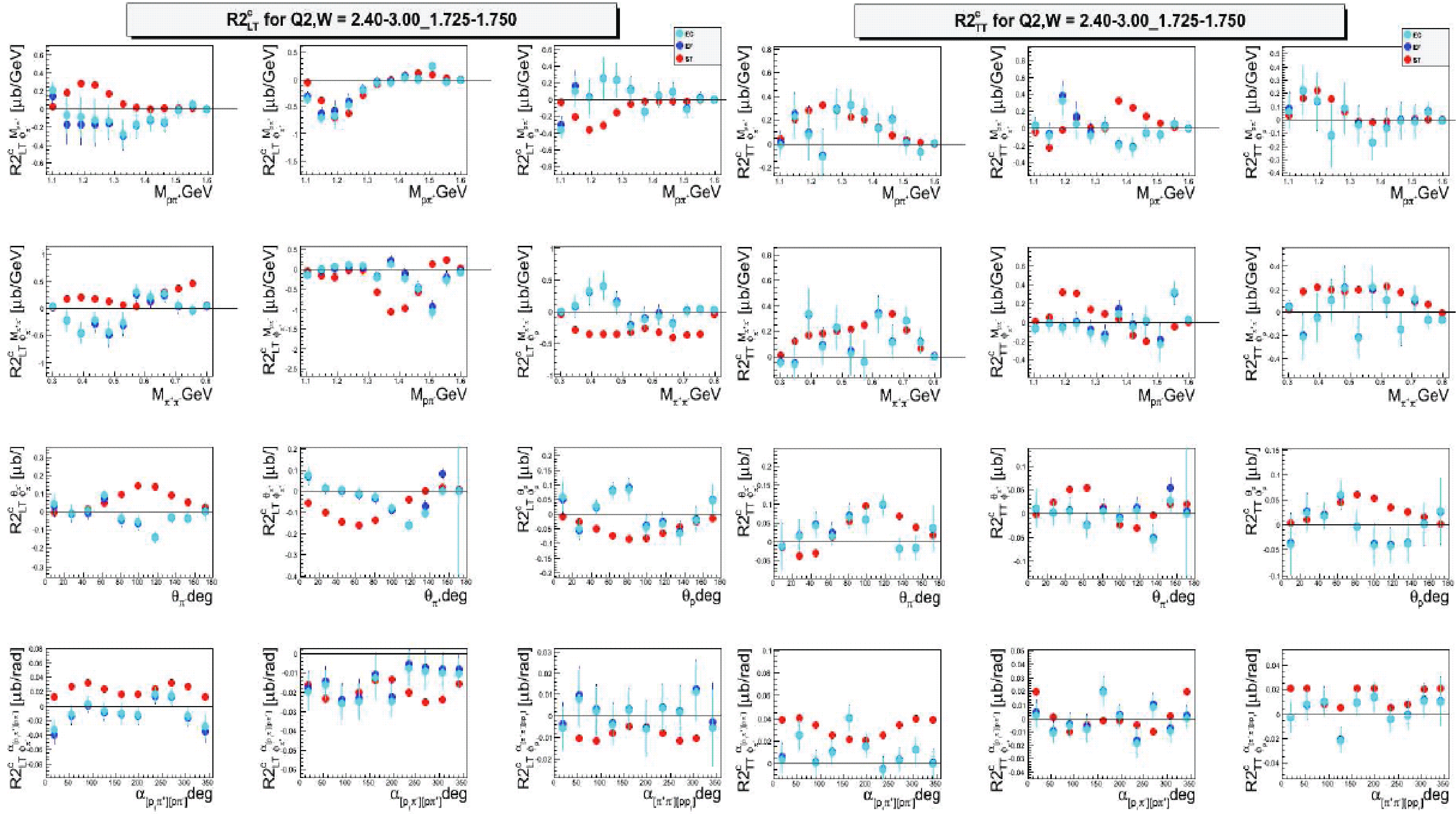


$$\left(\frac{d^2\sigma}{dX_{ij}d\phi_i}\right) = R2_T{}^{X_{ij}} + R2_L{}^{X_{ij}} + \underline{R2_{LT}{}^{c,X_{ij}}\cos\phi_i} + \underline{R2_{TT}{}^{c,X_{ij}}\cos 2\phi_i} + \delta_{X_{ij}\alpha_i}\left(R2_{LT}{}^{s,\alpha_i}\sin\phi_i + R2_{TT}{}^{s,\alpha_i}\sin 2\phi_i\right)$$

# φ-dependent Nππ Single-Differential Cross Sections

$Q^2, W$ bin $= [2.4, 3.0) GeV^2, [1.725, 1.750) GeV$ Arjun Trivedi

Chris McLauchlin extracts the beam helicity dependent differential cross sections.

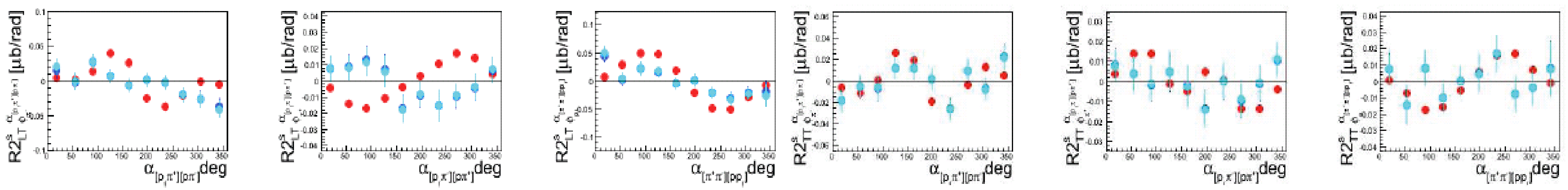

$$\left(\frac{d^2\sigma}{dX_{ij}\,d\phi_i}\right) = R2_T{}^{X_{ij}} + R2_L{}^{X_{ij}} + R2_{LT}{}^{c,X_{ij}}\cos\phi_i + R2_{TT}{}^{c,X_{ij}}\cos 2\phi_i + \delta_{X_{ij}\alpha_i}\left(\underline{R2_{LT}{}^{s,\alpha_i}\sin\phi_i} + \underline{R2_{TT}{}^{s,\alpha_i}\sin 2\phi_i}\right)$$

# Data-Driven Data Analyses

## Consistent Results

- Single meson production:
  - Unitary Isobar Model (UIM)
  - Fixed-*t* Dispersion Relations (DR)
- Double pion production:
  - Unitarized Isobar Model (JM)
- Coupled-Channel Approaches:
  - EBAC ⇒ Argonne-Osaka
  - JAW ⇒ Jülich-Athens-Washington ⇒ JüBo
  - BoGa ⇒ Bonn-Gatchina

Int. J. Mod. Phys. E, Vol. 22, 1330015 (2013) 1-99

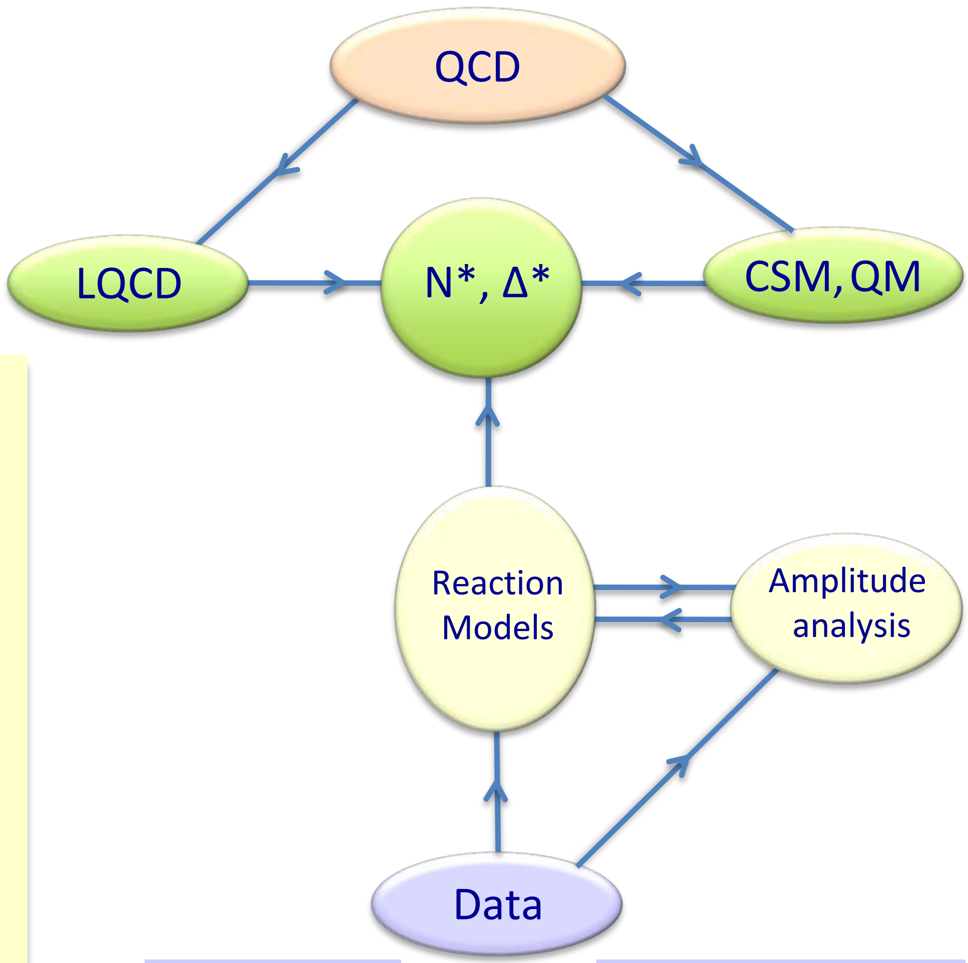


Hadronic production

Electromagnetic production

# N(1440)1/2$^+$ Couplings from CLAS

Viktor Mokeev

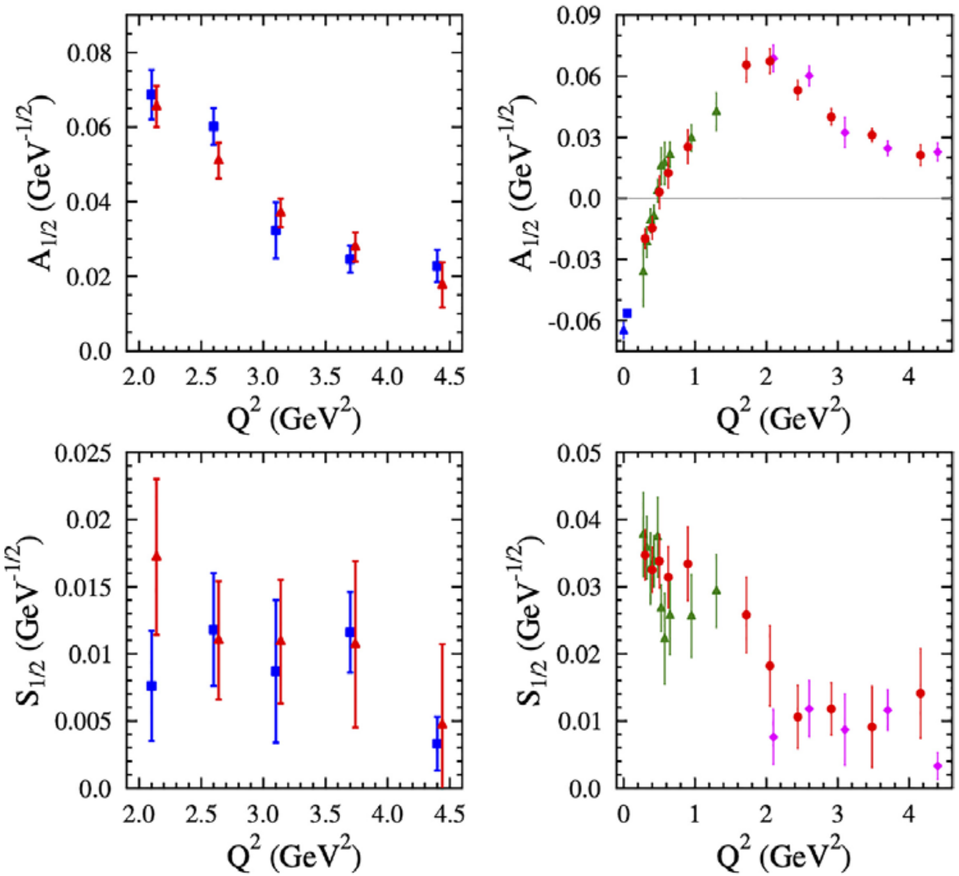


Consistent results are now obtained in the low-lying resonance region up to a $Q^2$ of 5 GeV$^2$ by independent analyses from the N$\pi$ differential cross sections, beam, target, and beam-target asymmetries (red triangles) and $p\pi^+\pi^-$ differential cross sections (blue squares).

All observables have fundamentally different mechanisms for the nonresonant background and underscore the capability of the reaction models to extract reliable resonance electrocouplings.

Phys. Rev. C 108, 025204 (2023) 1-26

# N(1520) 3/2⁻ Couplings from CLAS

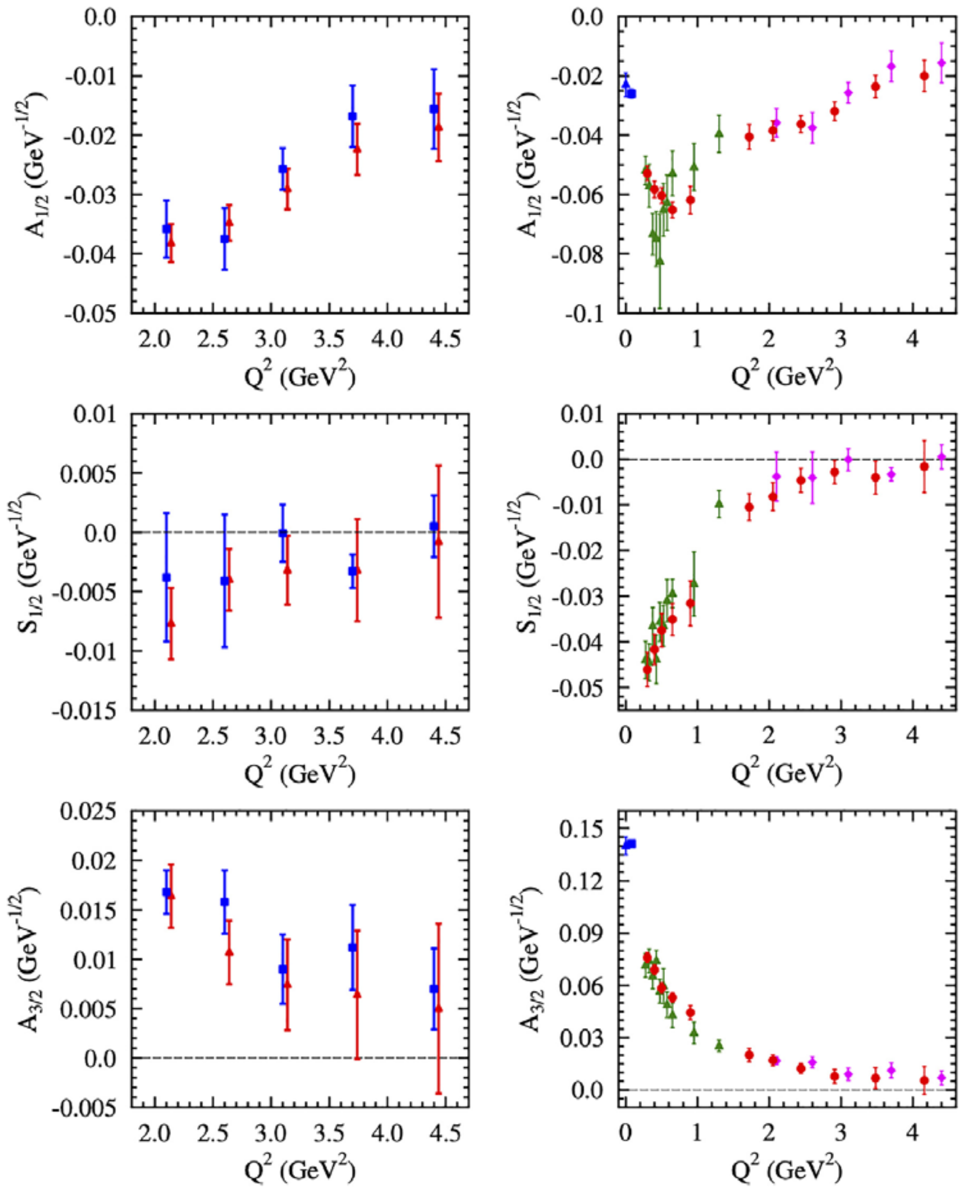


Viktor Mokeev

Consistent results are now obtained in the low-lying resonance region up to a $Q^2$ of 5 GeV$^2$ by independent analyses from the N$\pi$ differential cross sections, beam, target, and beam-target asymmetries (red triangles) and p$\pi^+\pi^-$ differential cross sections (blue squares).

All observables have fundamentally different mechanisms for the nonresonant background and underscore the capability of the reaction models to extract reliable resonance electrocouplings.

Phys. Rev. C 108, 025204 (2023) 1-26

# Δ(1600)3/2⁺ Form Factors in CSM Approach

Viktor Mokeev

CSM predictions of the Δ(1600)3/2⁺ electrocouplings

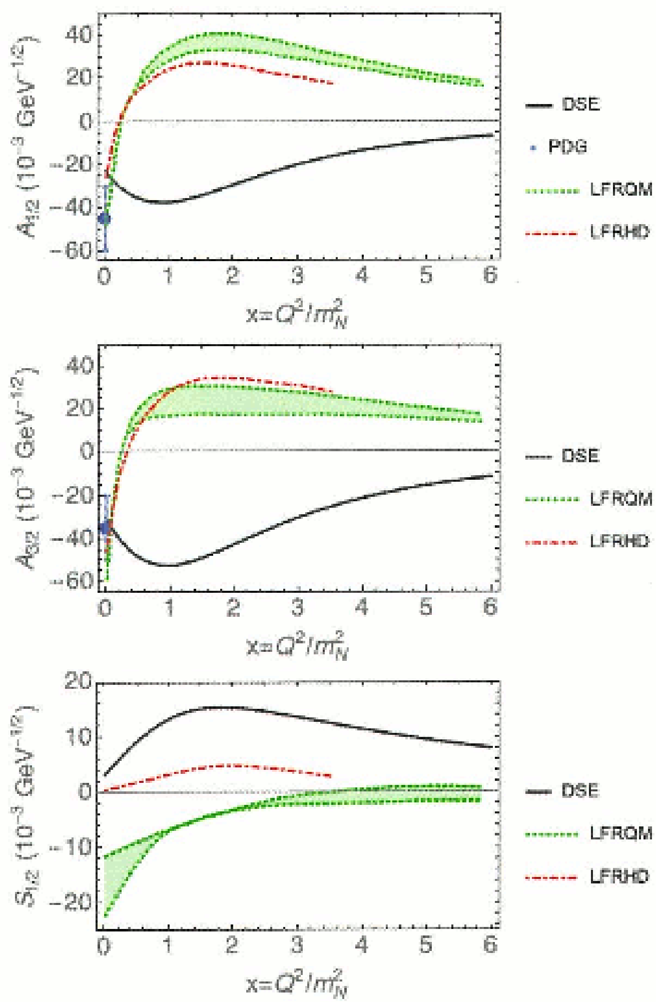


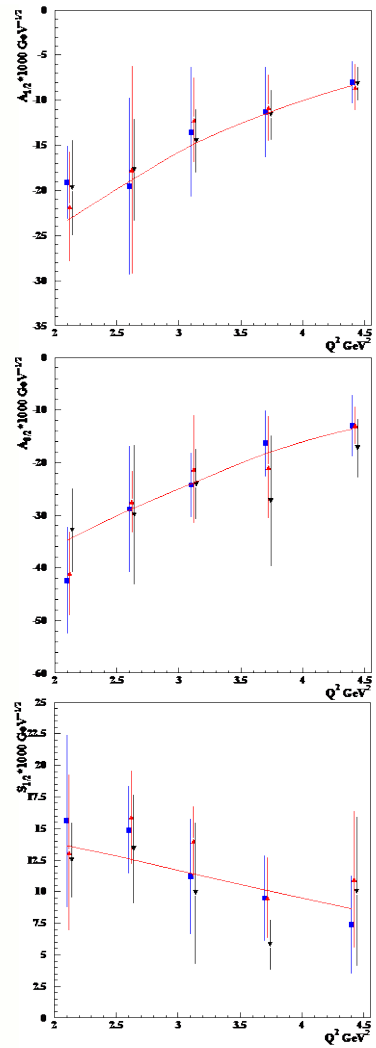


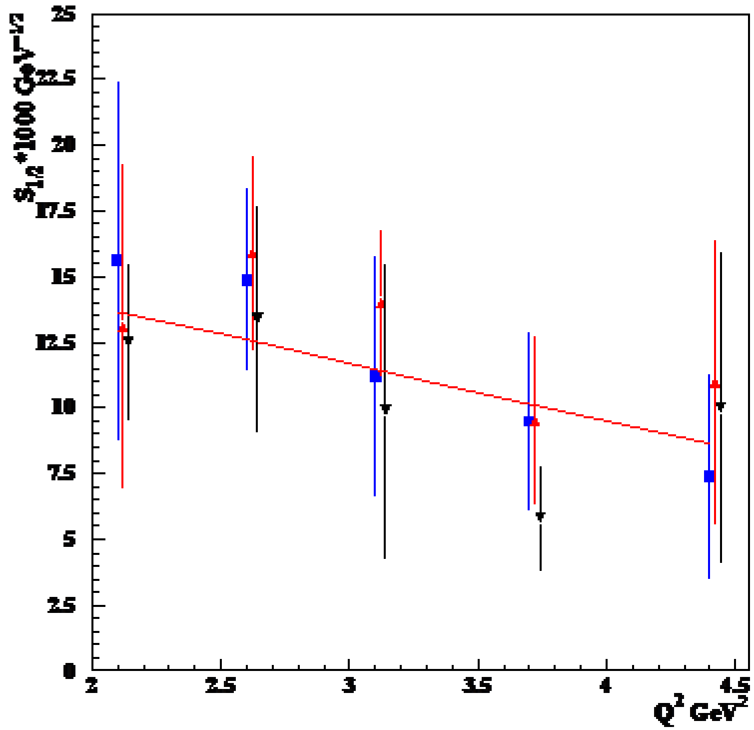


Spring 2022 analysis Arjun's $\pi^+\pi^-p$ differential cross sections for $2.0GeV^2<Q^2<5.0GeV^2$ within three W-intervals, 1.46GeV<W<1.56GeV, 1.51GeV<W<1.61GeV, and 1.56GeV<W<1.66GeV.

Ya Lu et al., PRD 100, 034001 (2019)

Phys. Rev. C 108, 025204 (2023) 1-26

# Emergence of Hadron Mass

Craig Roberts

k = $\sqrt{Q^2}/3$

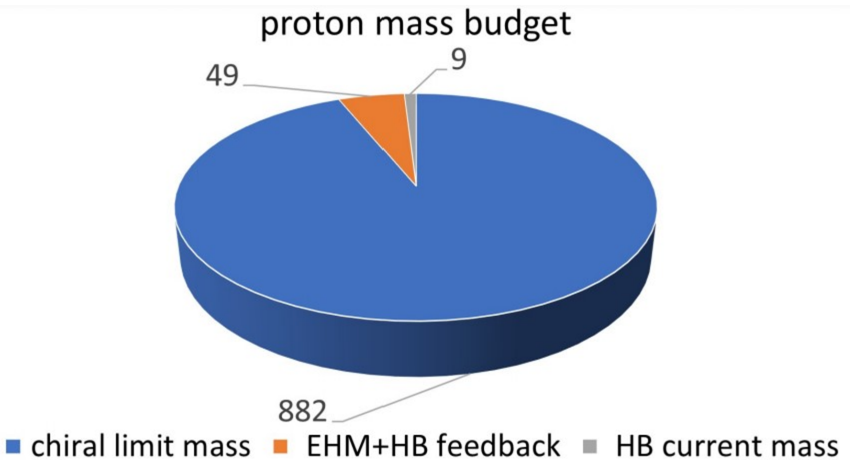


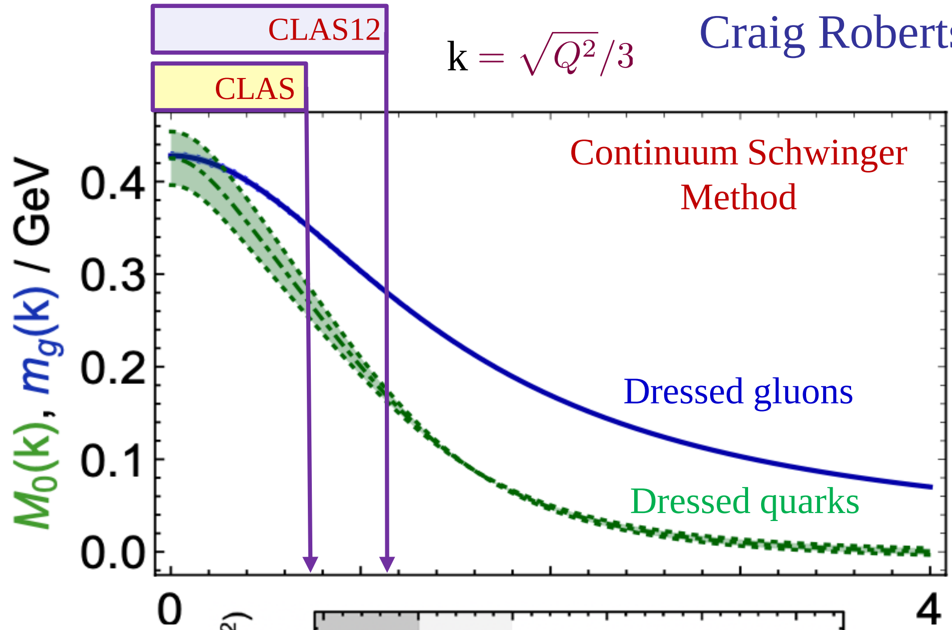


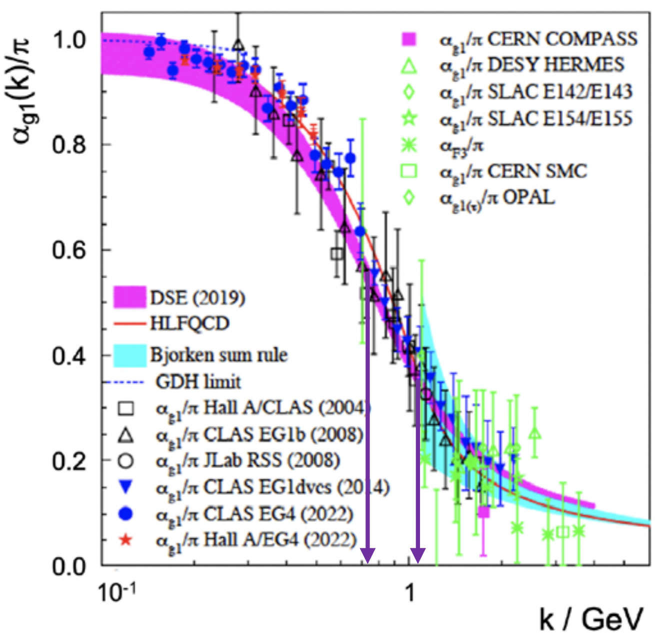


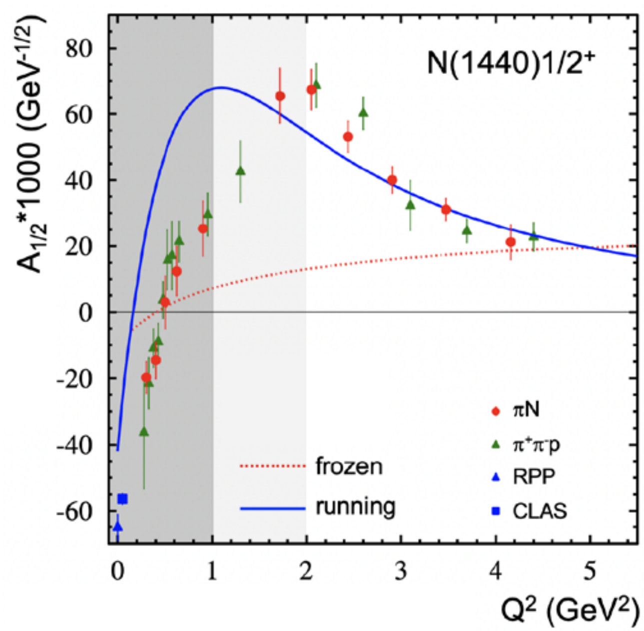

# CLAS12

# CLAS12

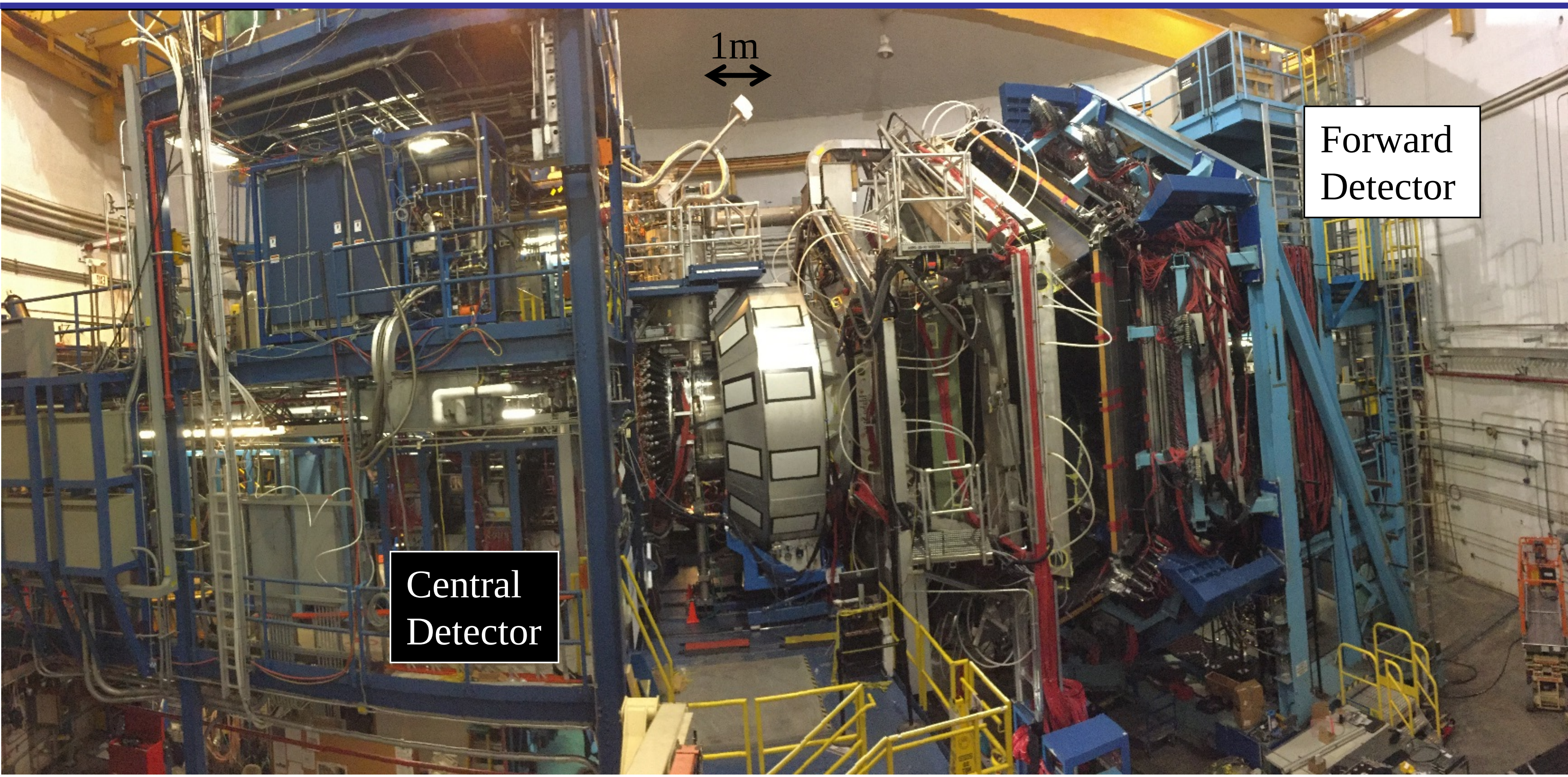


- Luminosity >$10^{35}$ $cm^{-2}s^{-1}$
- Hermeticity
- Polarization

- Baryon Spectroscopy
- Elastic Form Factors
- N → N* Form Factors

- GPDs and TMDs
- DIS and SIDIS
- Nucleon Spin Structure
- Color Transparency
- …

# Preliminary RGA CLAS12 Data Analysis: $p\pi^+\pi^-$

Krishna Neupane
CLAS12

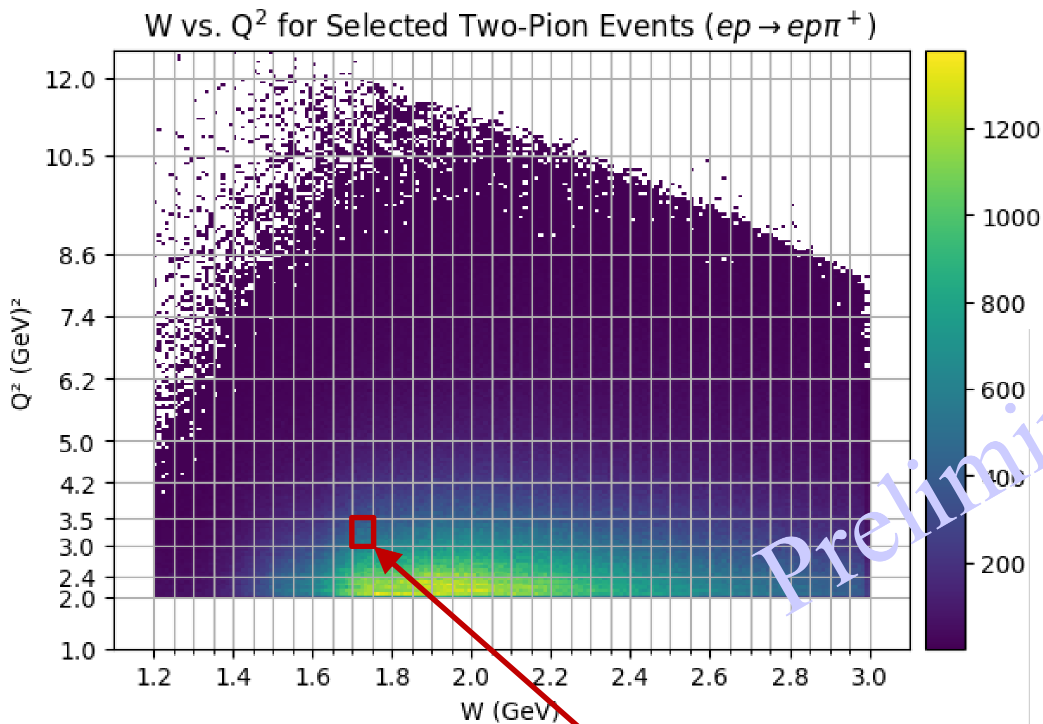


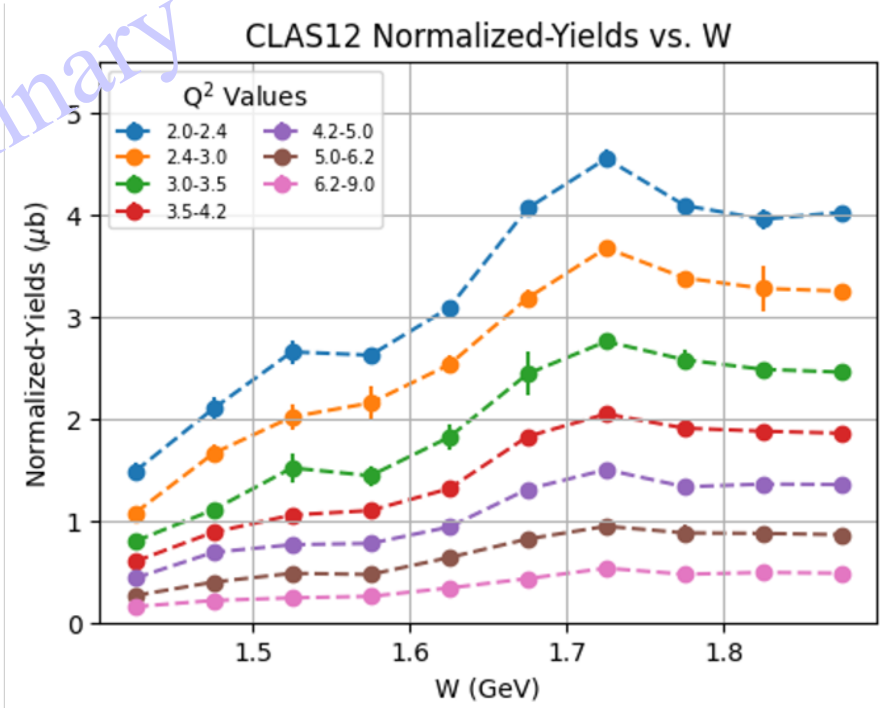


1.725 GeV < W < 1.75 GeV and 3 GeV$^2$ < Q$^2$ < 3.5 GeV$^2$

# Preliminary RGA CLAS12 Data Analysis: $p\pi^+\pi^-$

Krishna Neupane
CLAS12

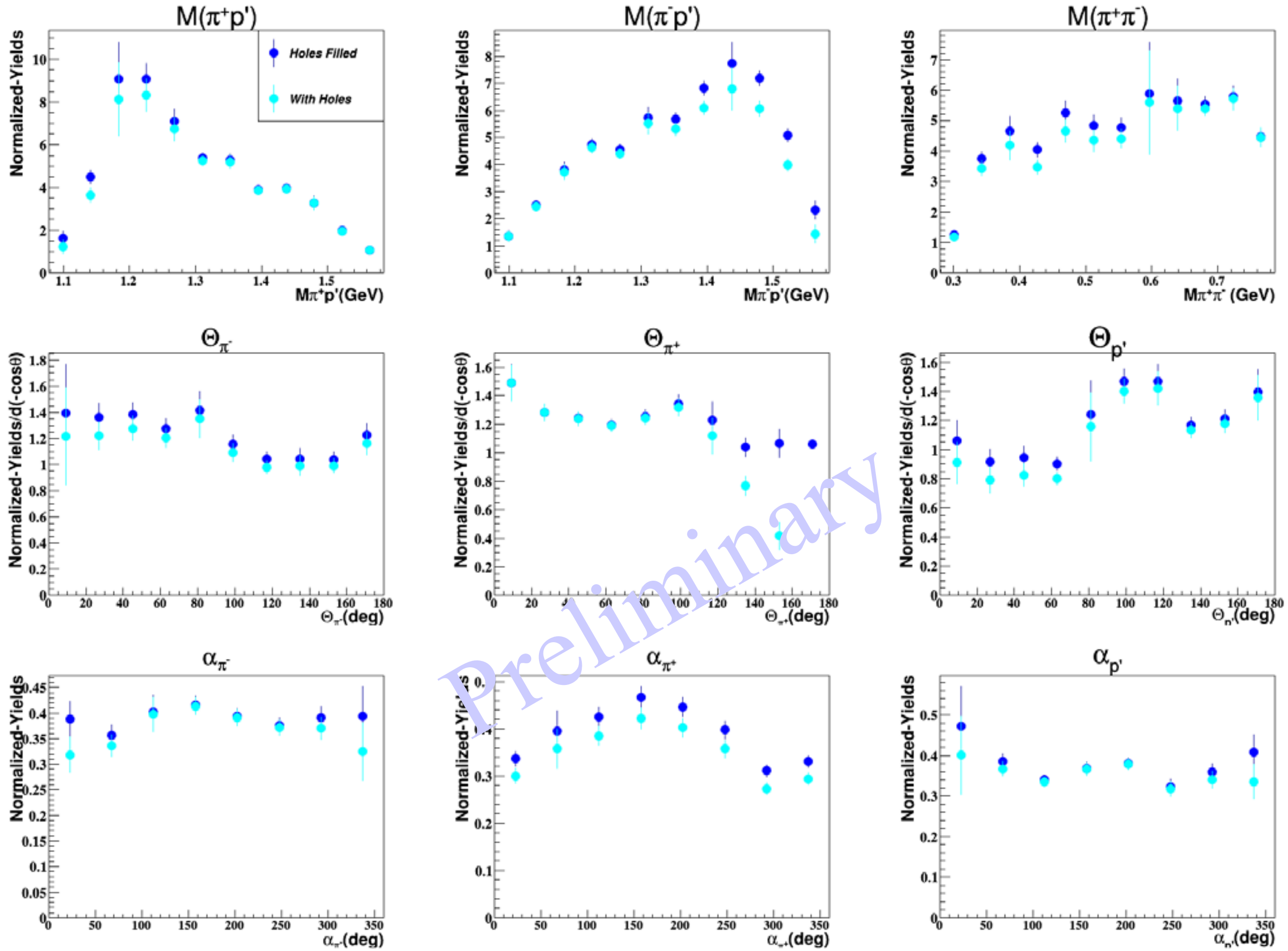


$1.725\ \text{GeV} < W < 1.75\ \text{GeV}$ and $3\ \text{GeV}^2 < Q^2 < 3.5\ \text{GeV}^2$

# φ-dependent Nππ Single-Differential Cross Sections

$Q^2, W \text{ bin} = [2.4, 3.0) GeV^2, [1.725, 1.750) GeV$

Arjun Trivedi
Evgeny Isupov

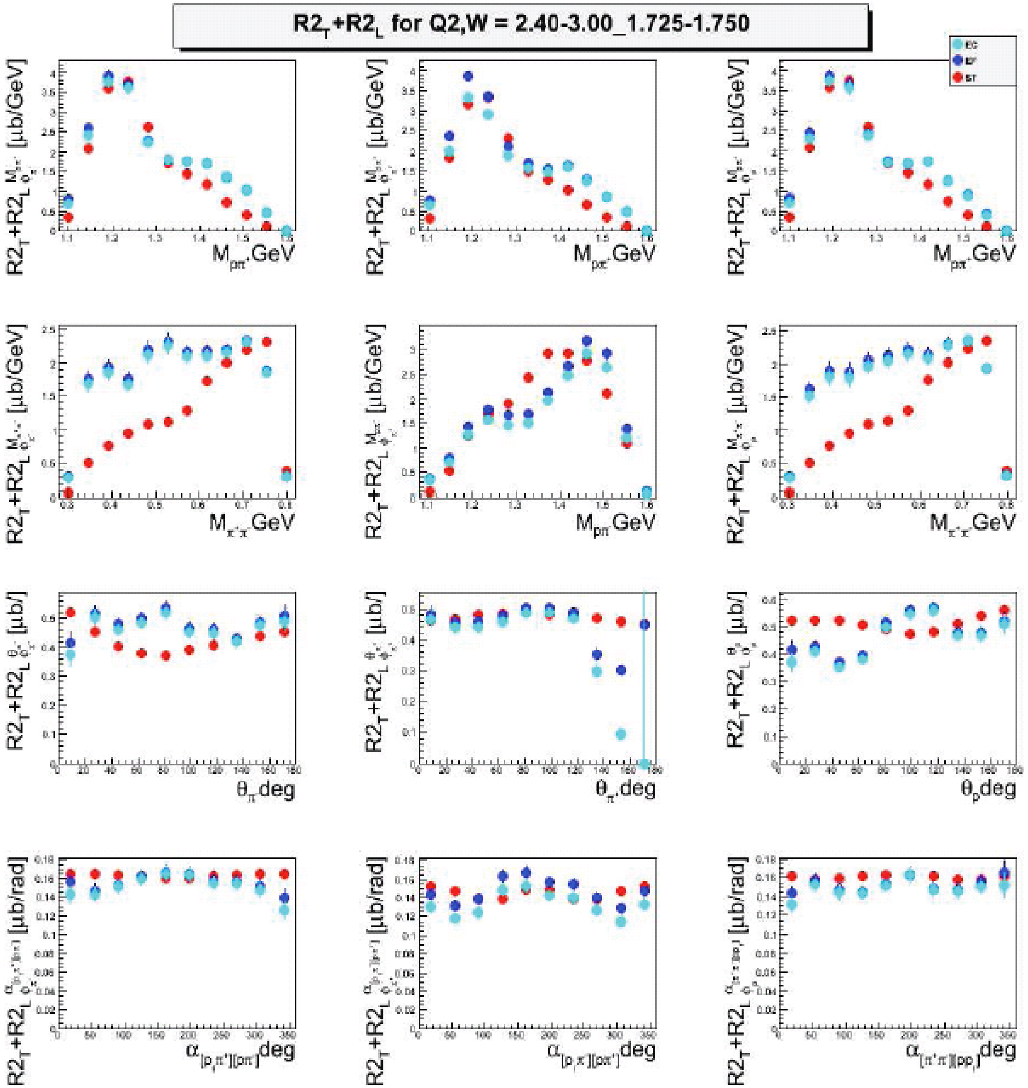


Krishna Neupane
CLAS12

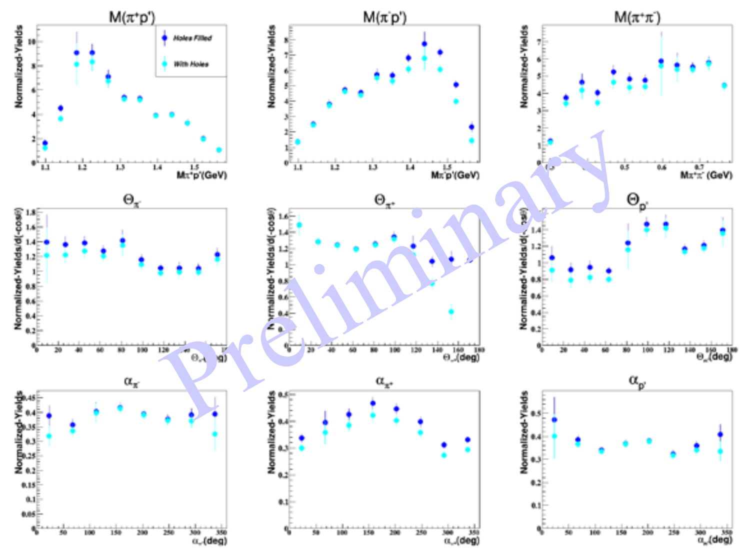


$$\left(\frac{d^2\sigma}{dX_{ij}\,d\phi_i}\right) = R2_T{}^{X_{ij}} + R2_L{}^{X_{ij}} + R2_{LT}{}^{c,X_{ij}} \cos\phi_i + R2_{TT}{}^{c,X_{ij}} \cos 2\phi_i + \delta_{X_{ij}\alpha_i}\left(R2_{LT}{}^{s,\alpha_i} \sin\phi_i + R2_{TT}{}^{s,\alpha_i} \sin 2\phi_i\right)$$

# CLAS22

# Achievable (W,Q2) Coverage at 22 GeV

Krishna Neupane

Simulated Reconstructed

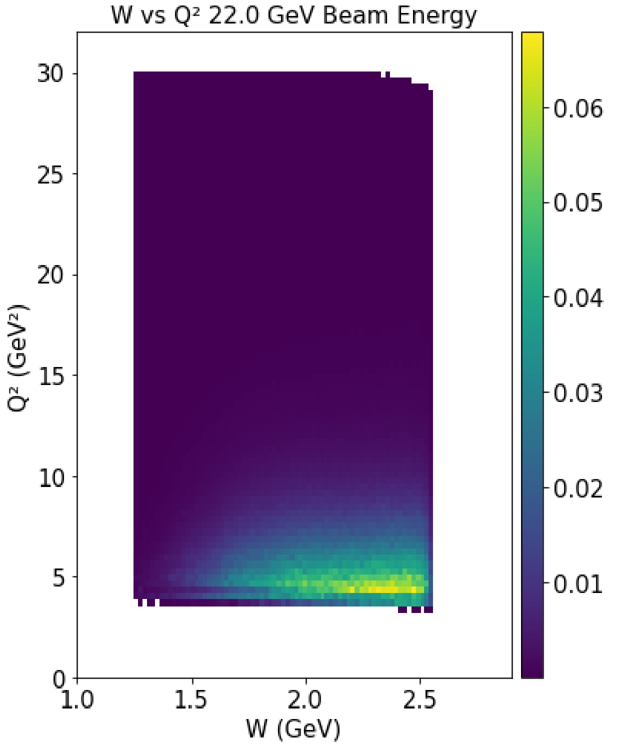


Simulated Reconstructed

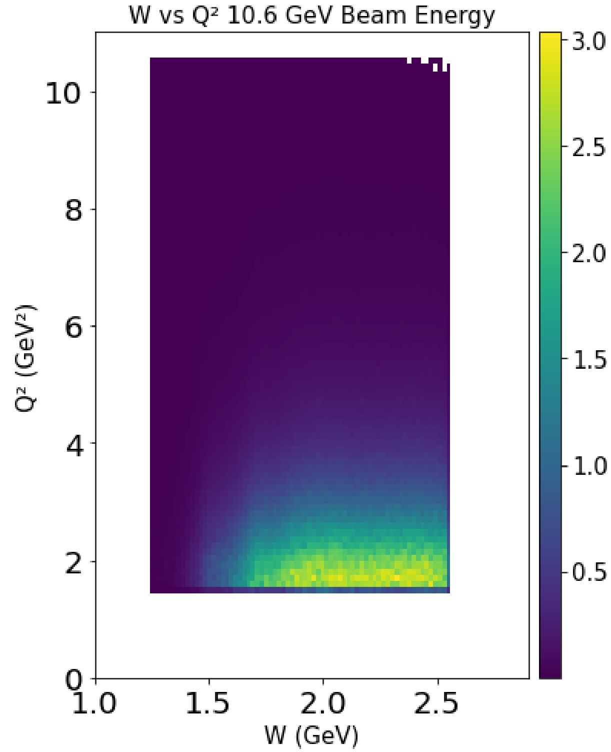


Measured Reconstructed

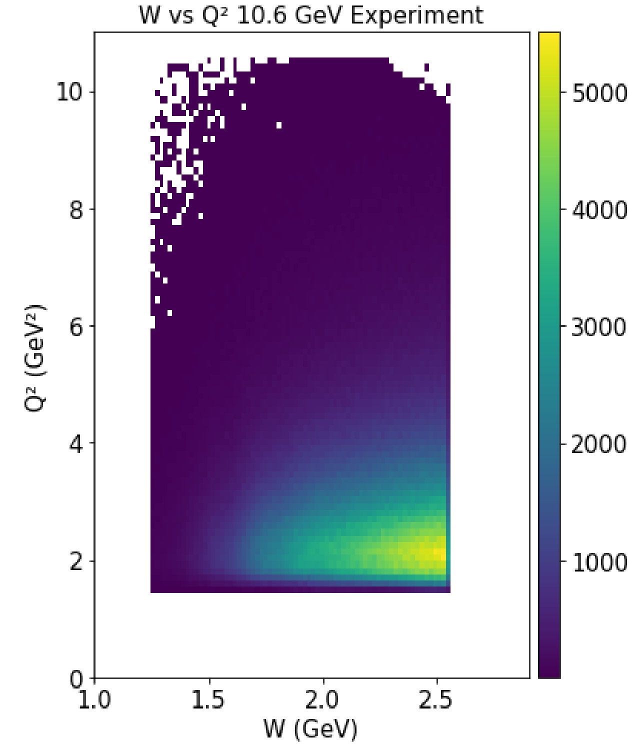


HSG is currently simulating:

- ✓ $p\pi^0, n\pi^+$ Maksim Davydov
- ✓ KY Dan Carman
- ✓ $p\pi^+\pi^-$ Krishna Neupane

- ➢ Comparison to RGA Fall 2018
- ➢ RGA inbending simulation
- ➢ Fully exclusive $p\pi^+\pi^-$

# TWOPEG Formfactor Extrapolation to 30 GeV²

Iuliia Skorodumina

$$\frac{d^5\sigma}{d^5\tau}(Q^2) = \frac{d^5\sigma}{d^5\tau}(0.65\ GeV^2) * \frac{F^2(Q^2)}{F^2(0.65\ GeV^2)}$$ with $F(Q^2) = \frac{1}{\left(1+\frac{Q^2}{0.7\ GeV^2}\right)}$

| point like | monopole | dipole |
|---|---|---|
| $F(Q^2) = 1$ | $F(Q^2) = \left(1+\frac{Q^2}{0.7\ GeV^2}\right)^{-1}$ | $F(Q^2) = \left(1+\frac{Q^2}{0.7\ GeV^2}\right)^{-2}$ |
| DIS | background | resonance excitation |

⚠ inclusive, semi-inclusive, exlusive:
each channel has a different $Q^2$ dependence ⚠

$$\frac{d^5\sigma}{d^5\tau}(Q^2) = \frac{d^5\sigma}{d^5\tau}(0.65\ GeV^2) * \frac{F^2(Q^2)}{F^2(0.65\ GeV^2)} * \frac{\left(F^2(Q^2)\right)^a}{\left(F^2(0.65\ GeV^2)\right)^b}$$

# Formfactor Extrapolation to 30 GeV$^2$

Krishna Neupane

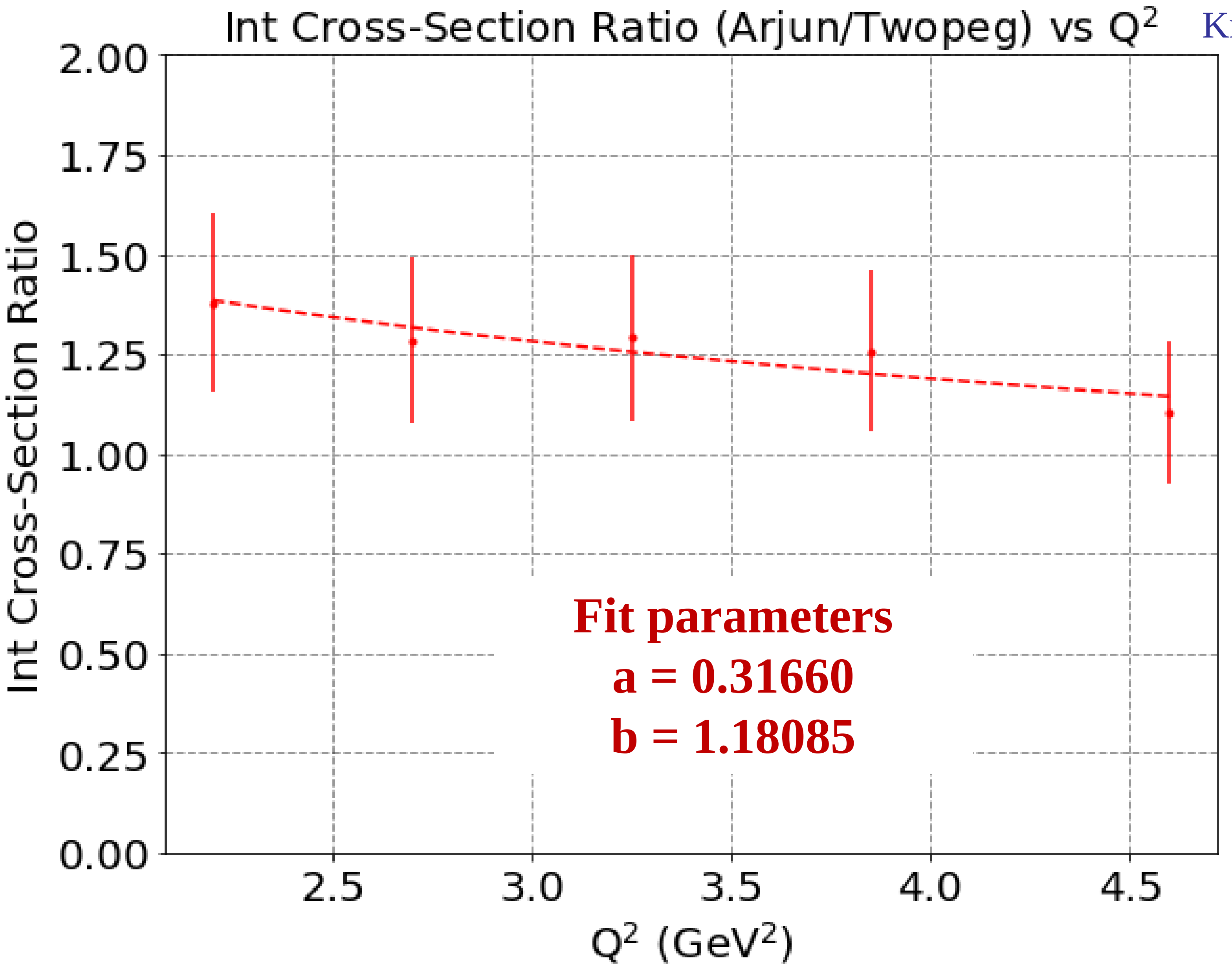


**Fit parameters**

**a = 0.31660**

**b = 1.18085**

# Formfactor Extrapolation to 30 GeV$^2$

Krishna Neupane

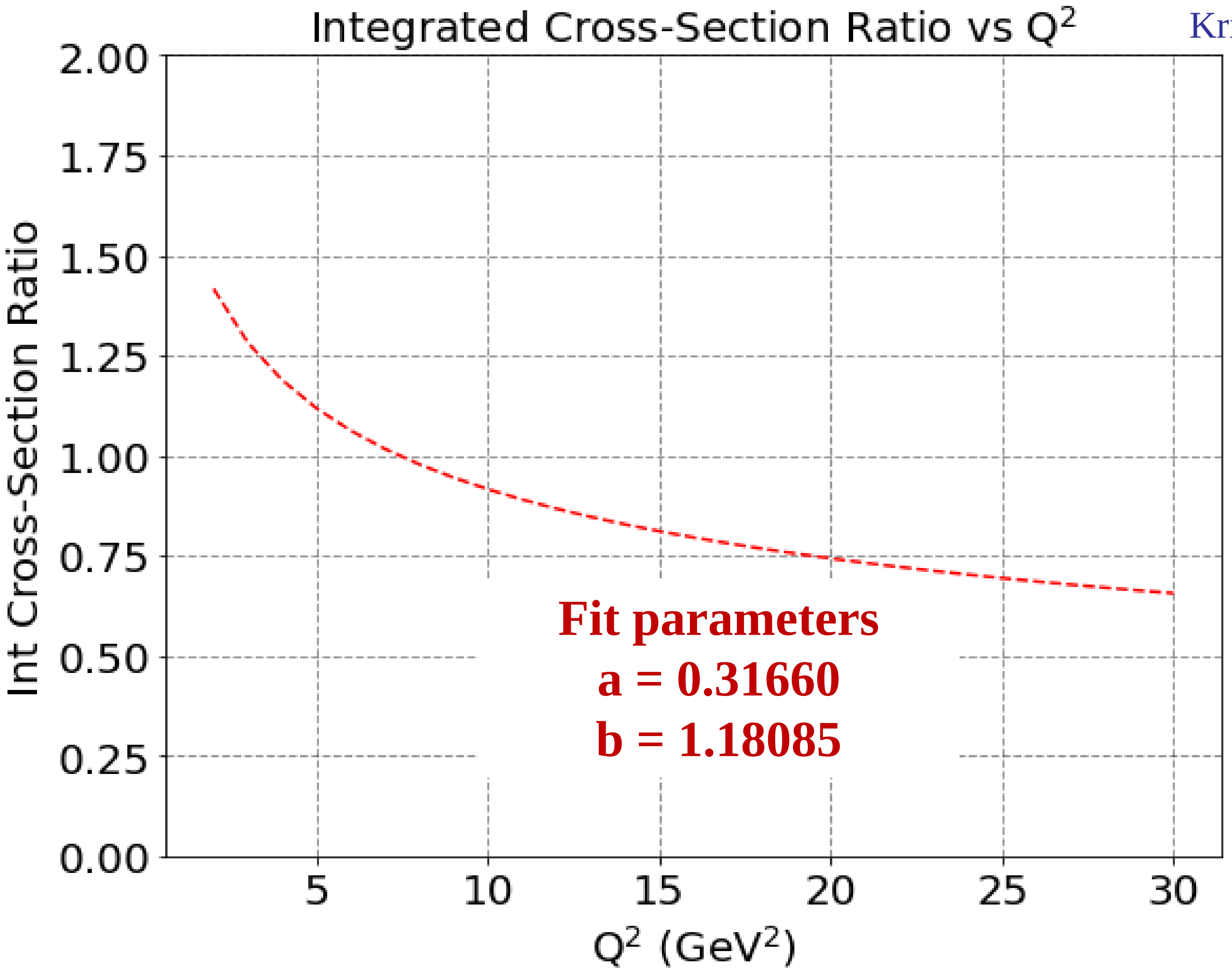


**Fit parameters**
**a = 0.31660**
**b = 1.18085**

# Formfactor Extrapolation to 30 GeV$^2$

Krishna Neupane

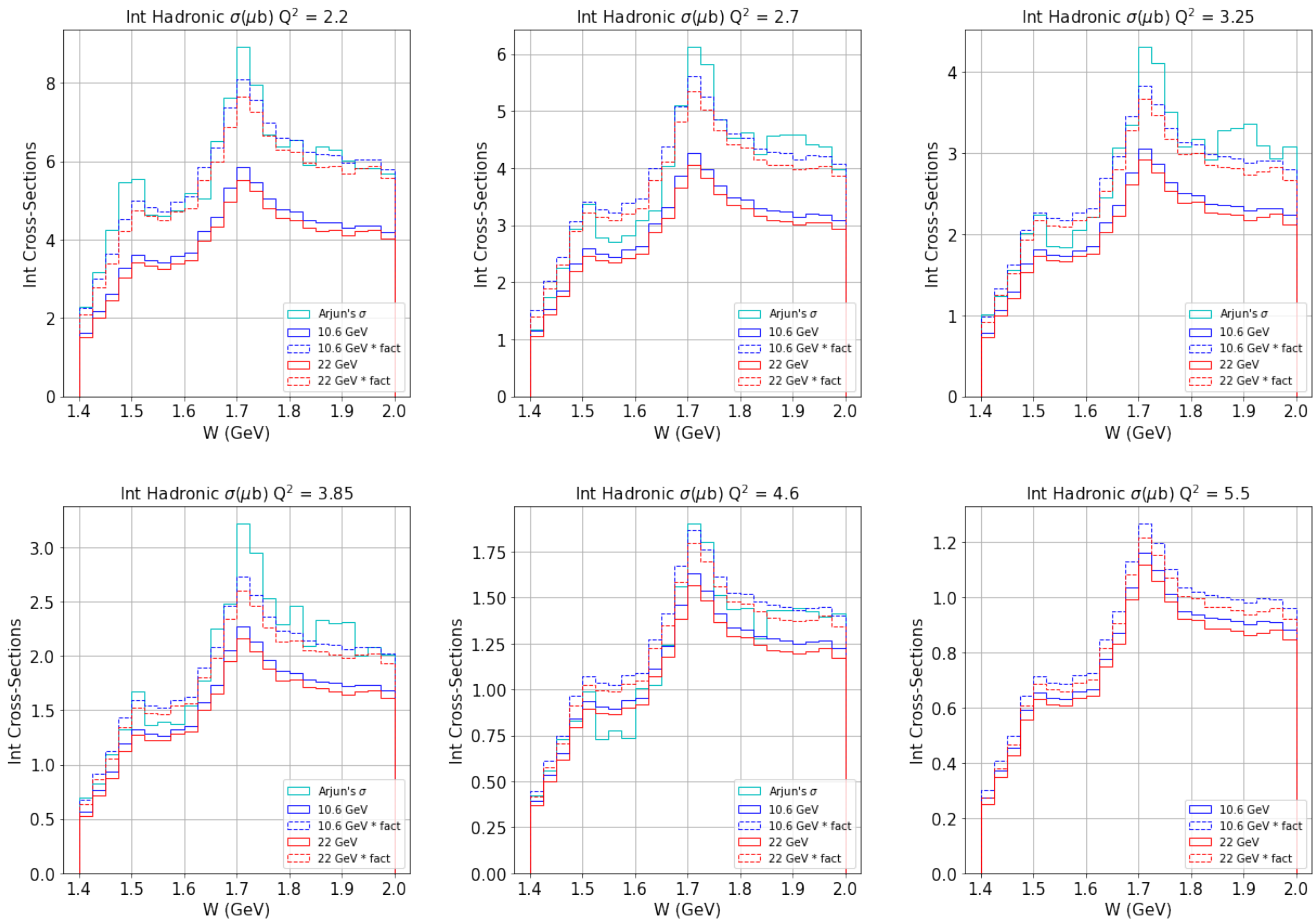

# Acceptance for Exclusive $p\pi^+\pi^-$ Final State

Alexis Osmond & Krishna Neupane

Simulated at 22 GeV Beam Energy

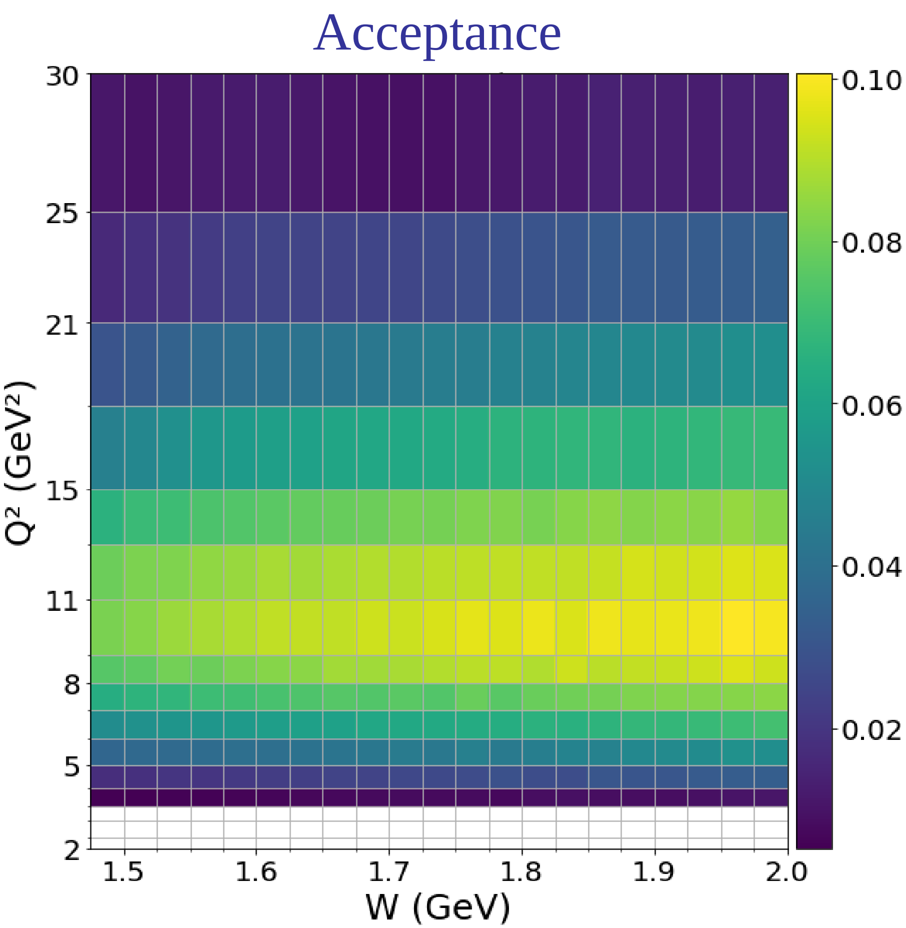


Simulated at 10.6 GeV Beam Energy

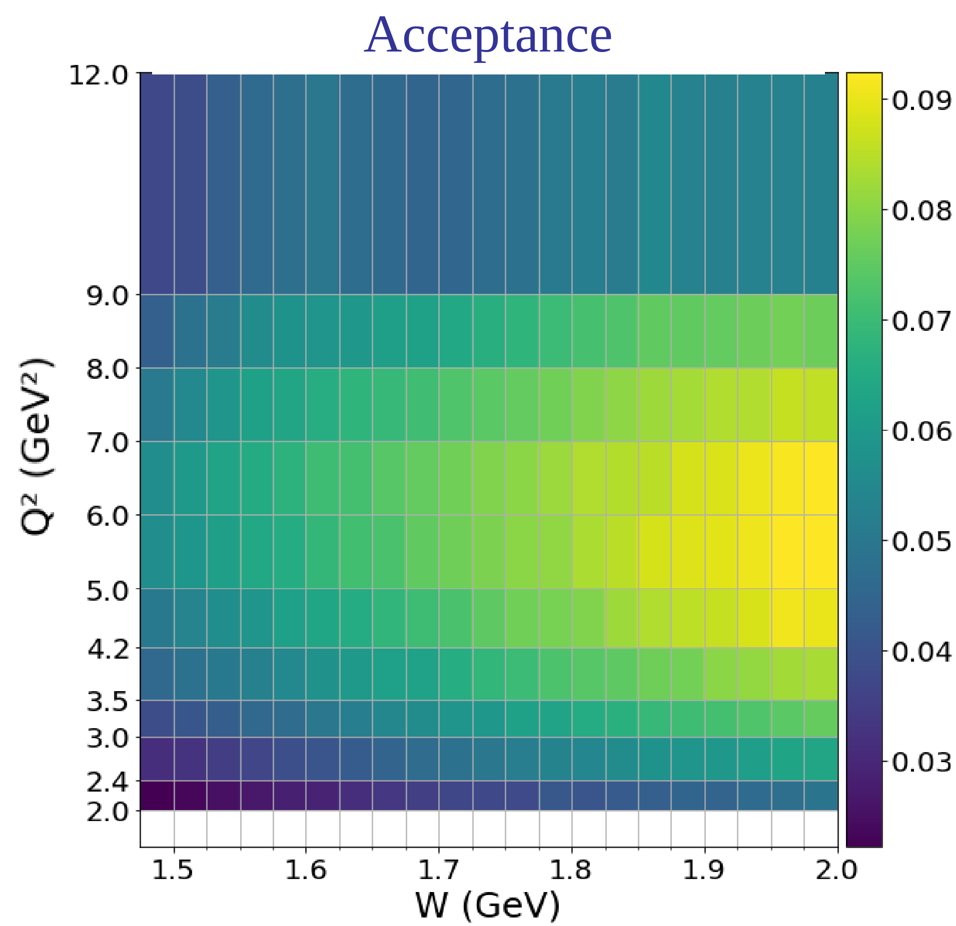

# Hadronic Cross Section for Exclusive $p\pi^+\pi^-$ Final State

Alexis Osmond & Krishna Neupane

Simulated at 22 GeV Beam Energy

Integrated Hadronic Cross Section (μb)

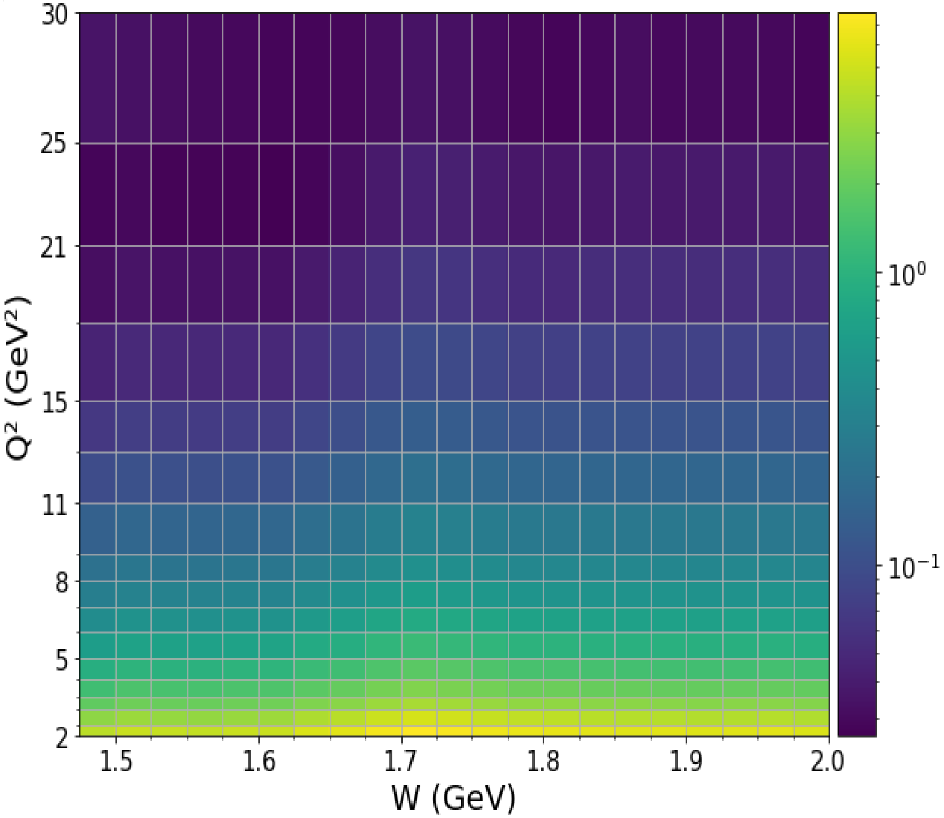


Simulated at 10.6 GeV Beam Energy

Integrated Hadronic Cross Section (μb)

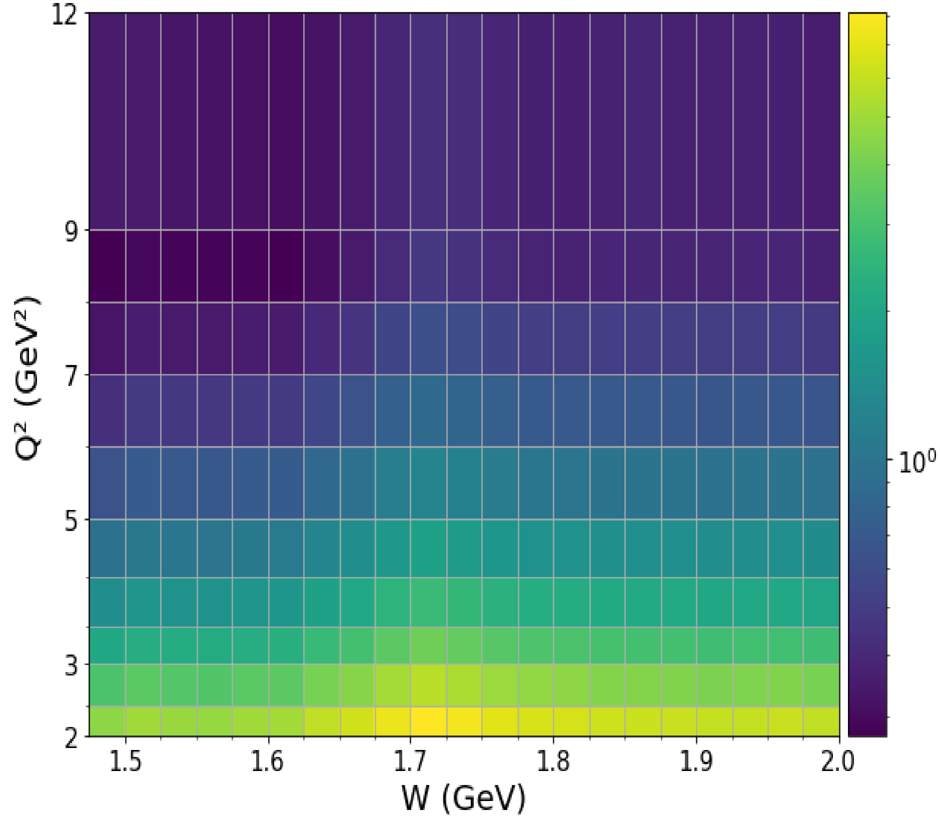

# Integrated Luminosity Needs for Exclusive $p\pi^+\pi^-$

Alexis Osmond & Krishna Neupane

## Simulated at 22 GeV Beam Energy

Needed Integrated Luminosity ($cm^{-2}$)

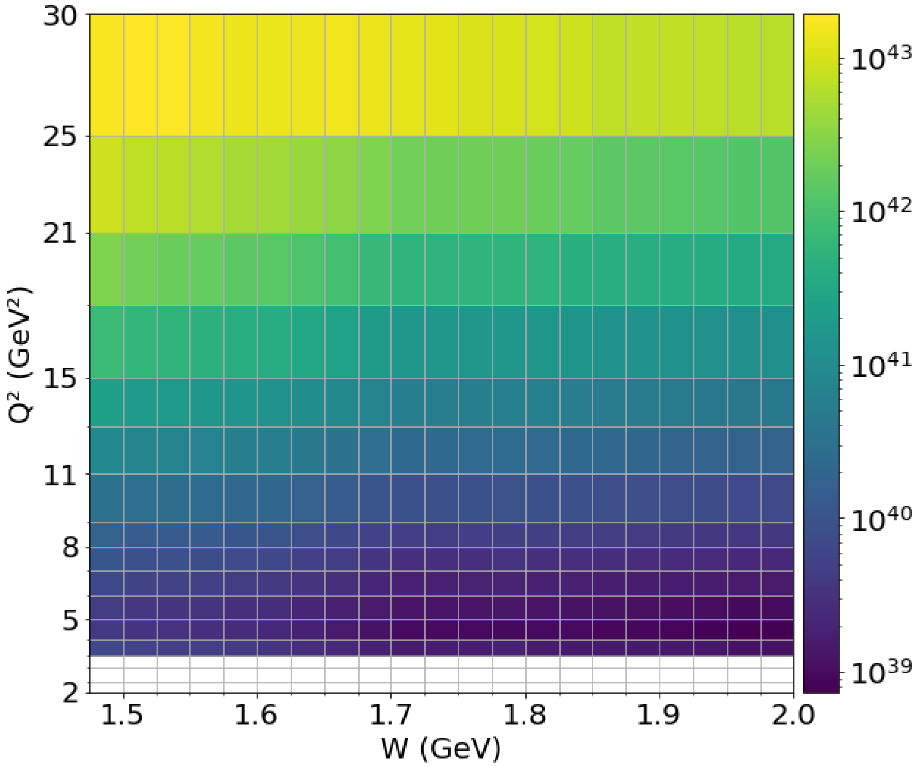


## Simulated at 10.6 GeV Beam Energy

Needed Integrated Luminosity ($cm^{-2}$)

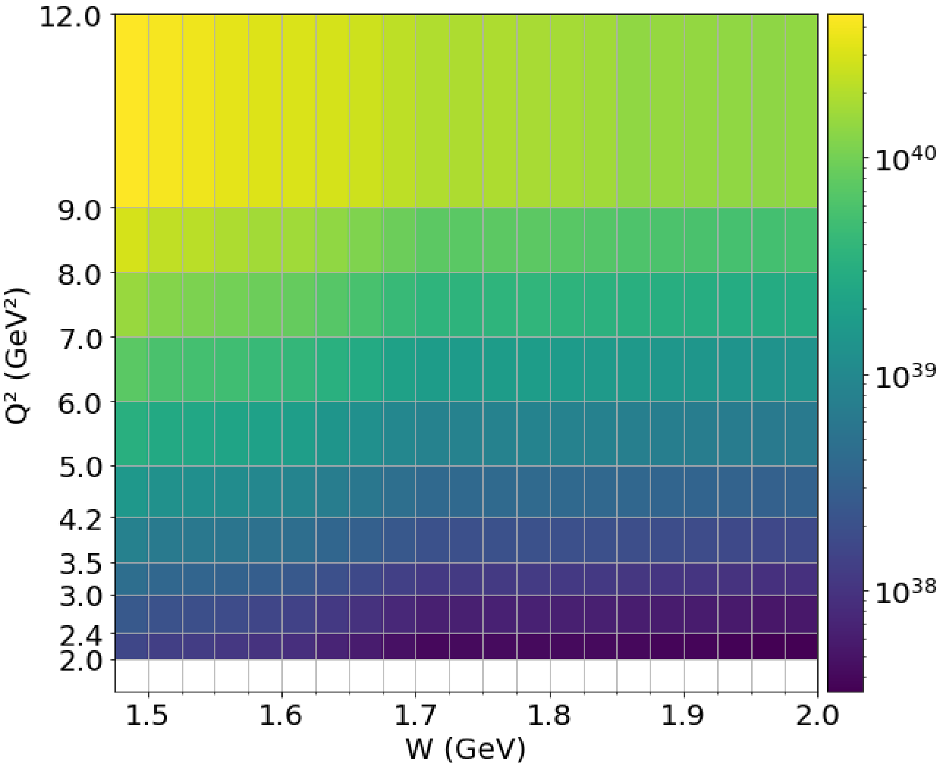

# Integrated Charge Needs for Exclusive $p\pi^+\pi^-$

Alexis Osmond & Krishna Neupane

Simulated at 22 GeV Beam Energy

Needed Integrated Charge (C)

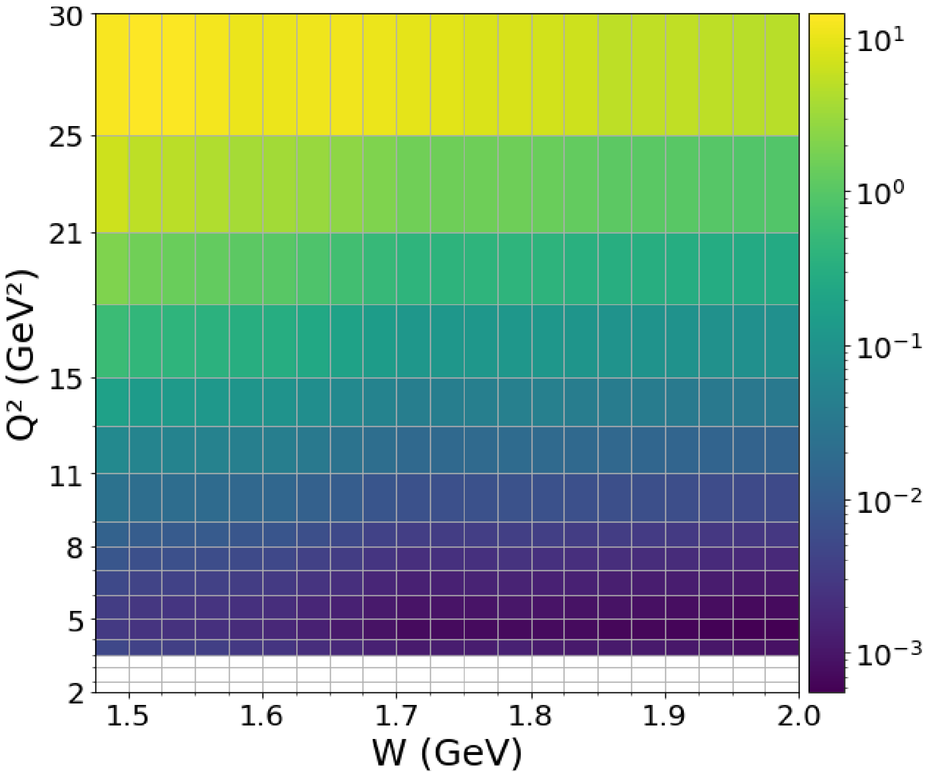


Simulated at 10.6 GeV Beam Energy

Needed Integrated Charge (C)

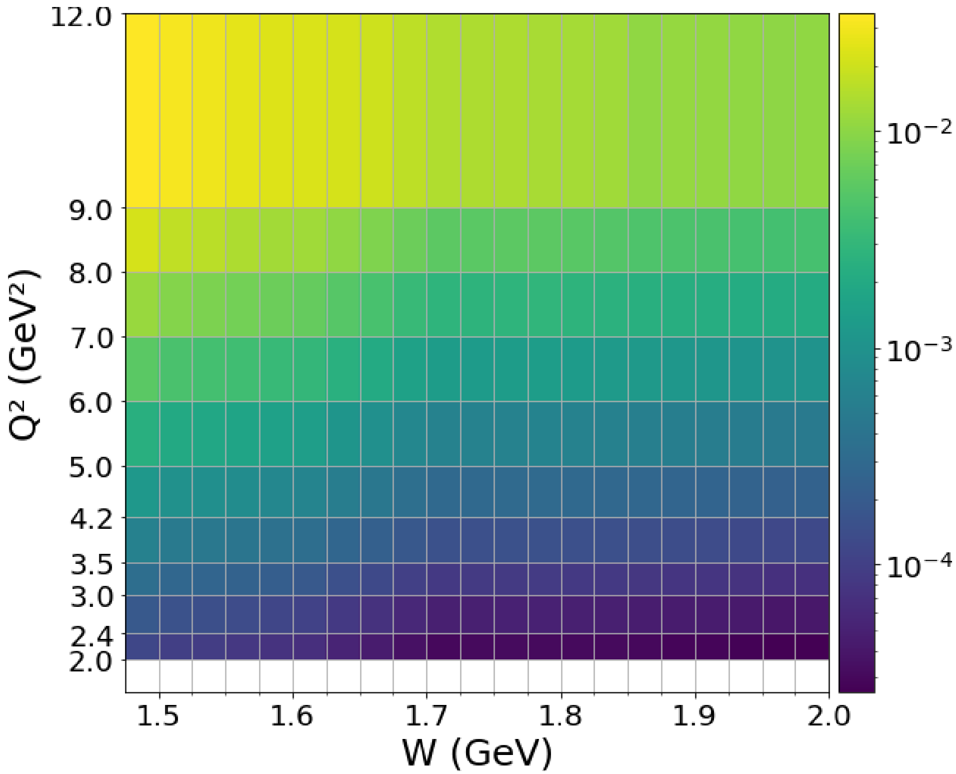

# Beam Time Needs for Exclusive $p\pi^+\pi^-$

Alexis Osmond & Krishna Neupane

Based on RGA Fall 2018 Luminosity of 5.96 $10^{34}$ $cm^{-2}$ $s^{-1}$ at 45 nA and 5 cm $LH_2$

Simulated at 22 GeV Beam Energy

Needed Years at $5.96 \cdot 10^{34}$ ($cm^{-2}$ $s^{-1}$)

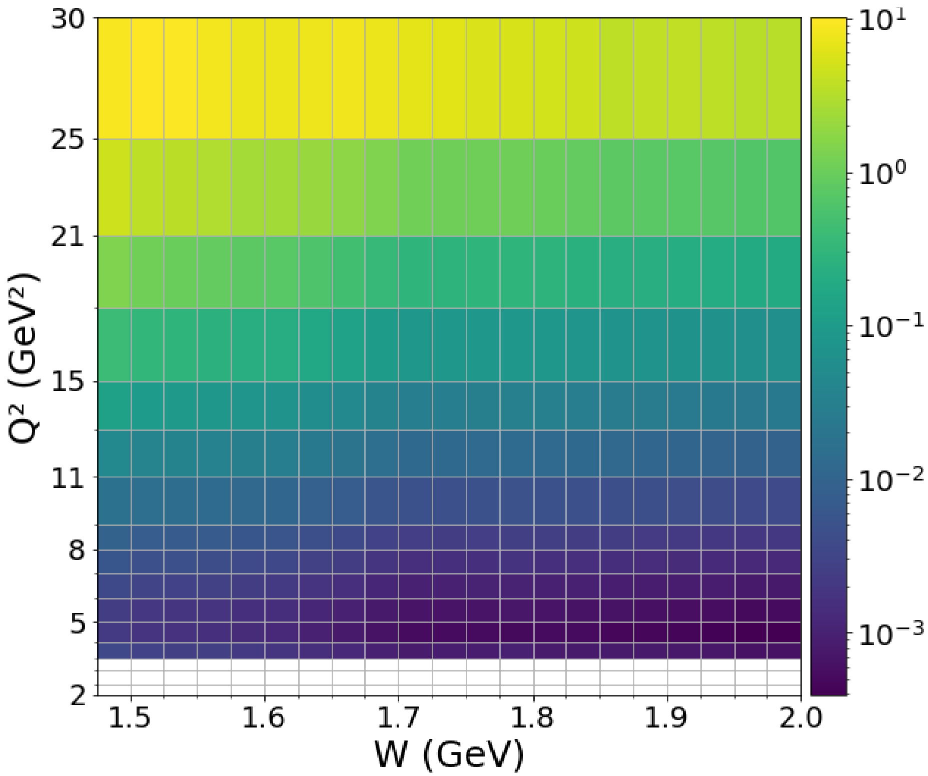


Simulated at 10.6 GeV Beam Energy

Needed Years at $5.96 \cdot 10^{34}$ ($cm^{-2}$ $s^{-1}$)

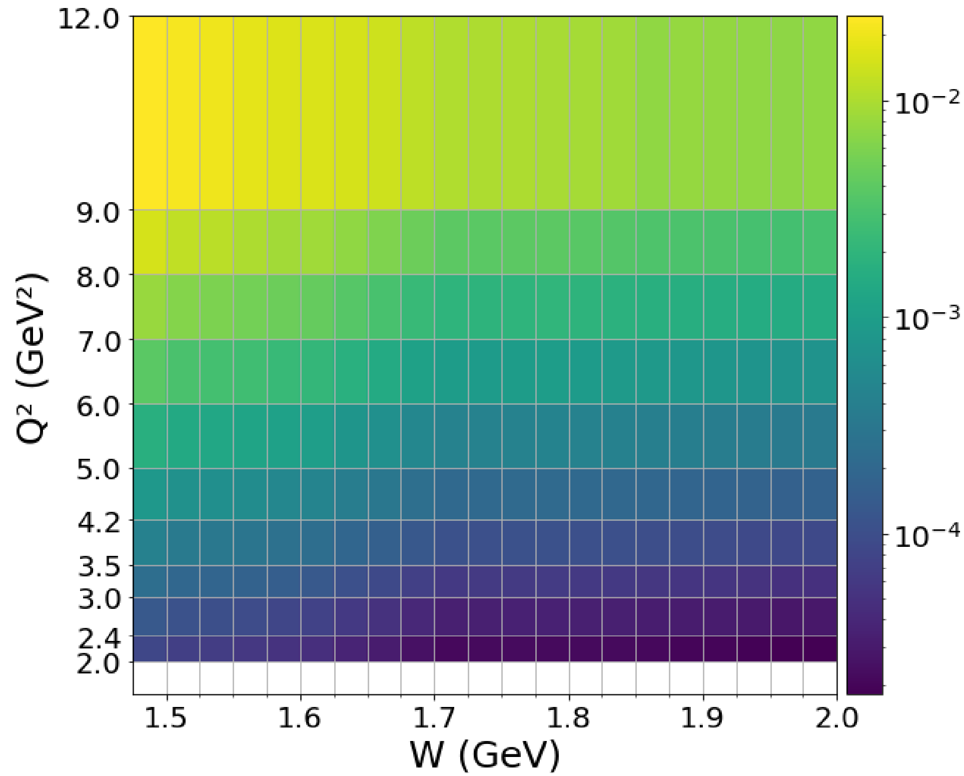


Implementing all analysis cuts (3/2), Golden Run Selection (3), PAC Days (2)

➡ 8 (16) years at $5.96 \cdot 10^{34}$ $cm^{-2}$ $s^{-1}$ or 11 (22) month at $5 \cdot 10^{35}$ $cm^{-2}$ $s^{-1}$

# Beam Time Needs for Exclusive $p\pi^+\pi^-$

Alexis Osmond & Krishna Neupane

Based on RGA Fall 2018 Luminosity of 5.96 $10^{34}$ $cm^{-2}$ $s^{-1}$ at 45 nA and 5 cm $LH_2$

Simulated at 22 GeV Beam Energy

Simulated at 10.6 GeV Beam Energy

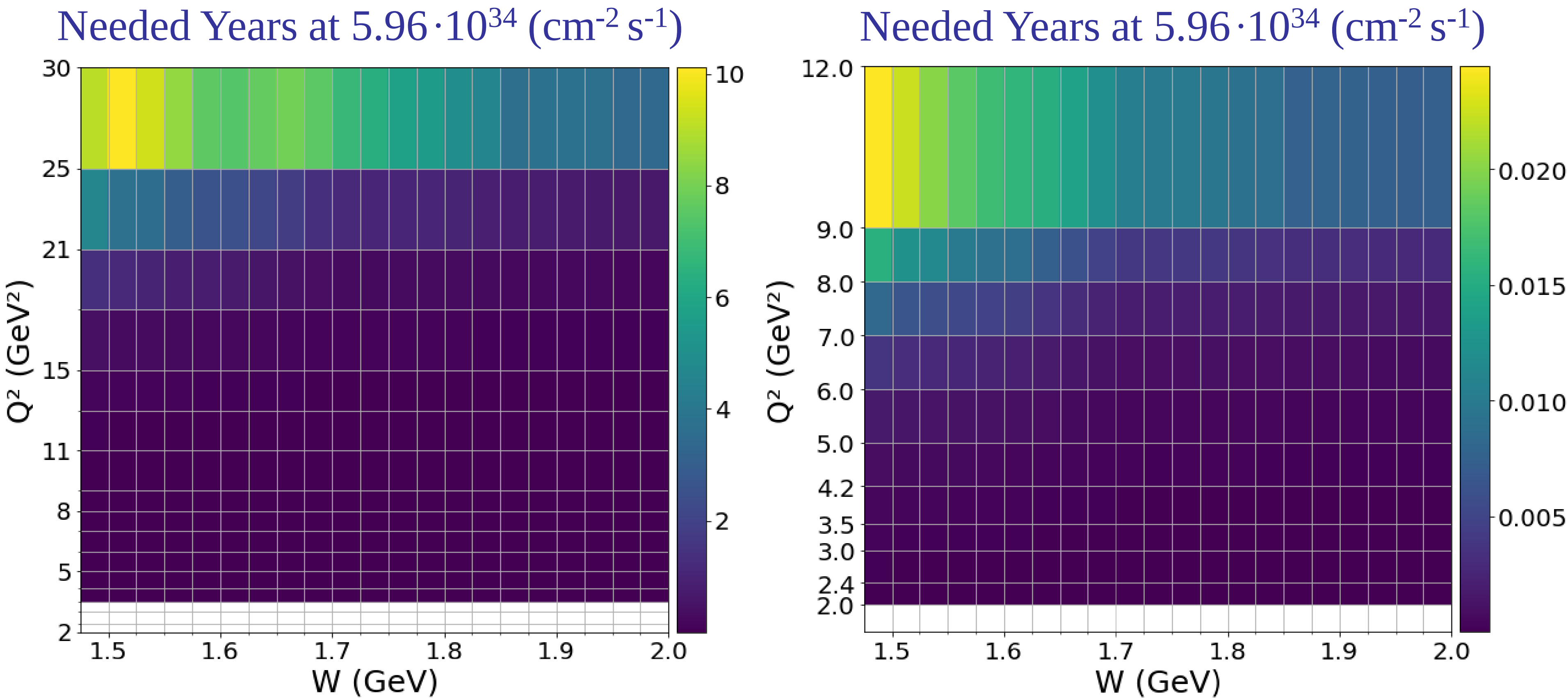


Implementing all analysis cuts (3/2), Golden Run Selection (3), PAC Days (2)

➡ 8 (16) years at 5.96·$10^{34}$ $cm^{-2}$ $s^{-1}$ or 11 (22) month at 5·$10^{35}$ $cm^{-2}$ $s^{-1}$

# Hadron Structure Needs for CLAS22

| | $Q^2$-coverage of electrocouplings | Range of quark momenta k | Fraction of dressed quark mass at $k<k_{max}$ |
|---|---|---|---|
| CLAS | < 5 GeV$^2$ | < 0.8 GeV | 30% |
| CLAS12 | < 12 GeV$^2$ | < 1.2 GeV | 50% |
| CLAS22 | < 35 GeV$^2$ | < 2.0 GeV | 90% |

- Beam energy 22 GeV
- Nearly $4\pi$ acceptance

**EHM**

$k = \sqrt{Q^2}/3$

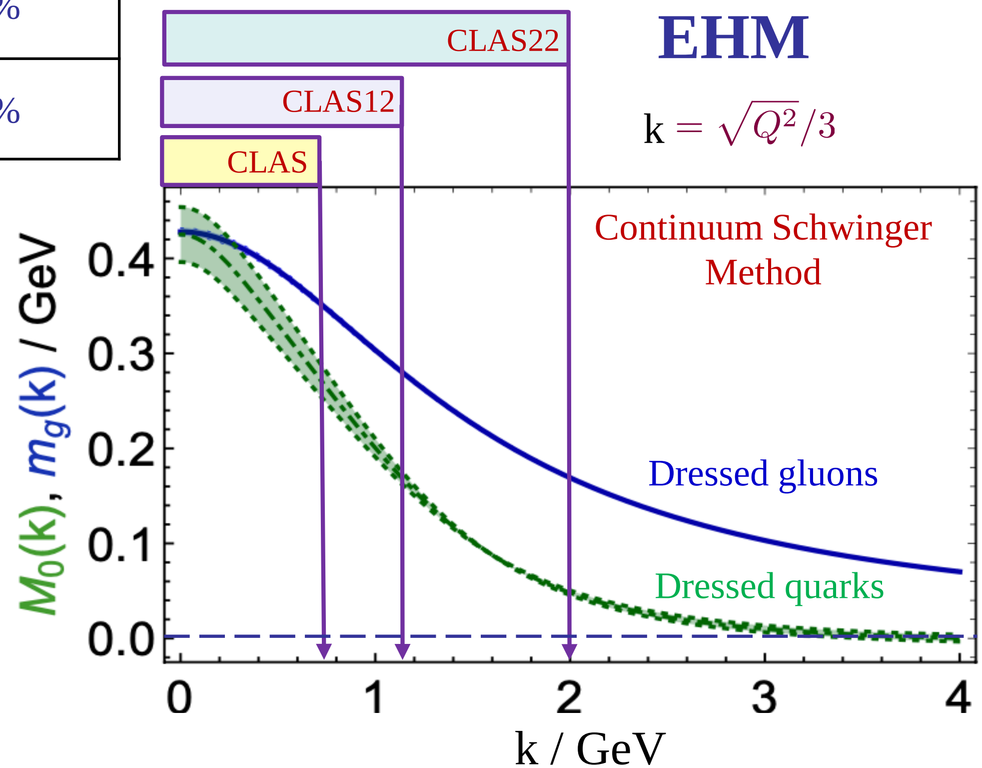


Increasing knowledge on running dressed quark mass from the results on $\gamma_v pN^*$ electrocouplings.

Measured $\gamma_v pN^*$ electrocouplings of most prominent N* states of different structure will provide sound evidence for understanding how the dominant part of the hadron mass and the N* structure itself emerge from QCD and will make CEBAF@22 GeV the ultimate QCD-facility at the luminosity frontier.

Luminosity “frontier” is the *unique* advantage of JLab.

# Hadron Structure Needs for CLAS22

| | $Q^2$-coverage of electrocouplings | Range of quark momenta k | Fraction of dressed quark mass at $k<k_{max}$ |
|---|---|---|---|
| CLAS | < 5 $GeV^2$ | < 0.8 GeV | 30% |
| CLAS12 | < 12 $GeV^2$ | < 1.2 GeV | 50% |
| CLAS22 | < 35 $GeV^2$ | < 2.0 GeV | 90% |

- Beam energy 22 GeV
- Nearly $4\pi$ acceptance

Increasing knowledge on running dressed quark mass from the results on $\gamma_v pN^*$ electrocouplings.

Measured $\gamma_v pN^*$ electrocouplings of most prominent N* states of different structure will provide sound evidence for understanding how the dominant part of the hadron mass and the N* structure itself emerge from QCD and will make CEBAF@22 GeV the ultimate QCD-facility at the luminosity frontier.

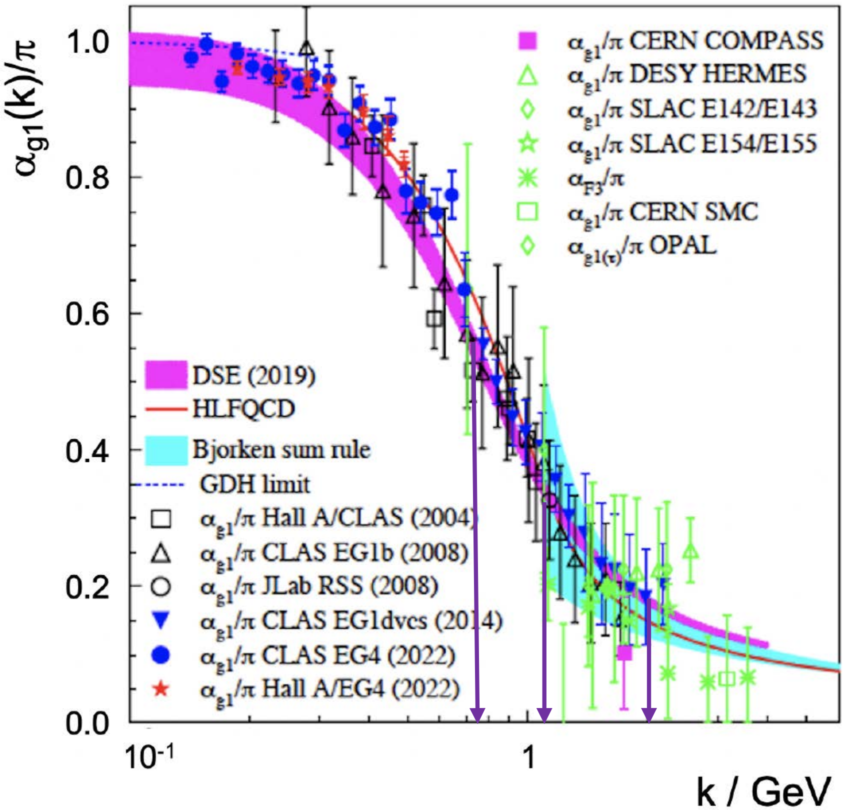


Luminosity “frontier” is the *unique* advantage of JLab.

# Hadron Structure Needs for CLAS22

- Beam energy 22 GeV
- Nearly 4π acceptance

- High luminosity detector
- High momentum resolution
- Studies of exclusive reactions

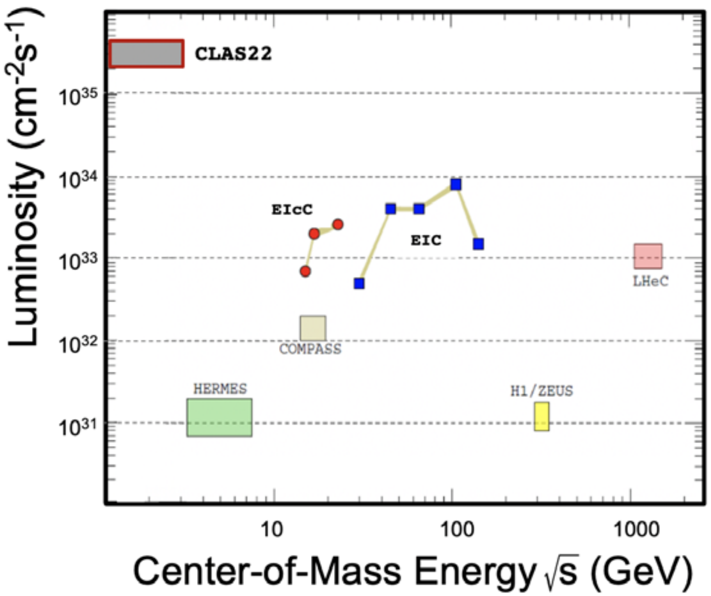


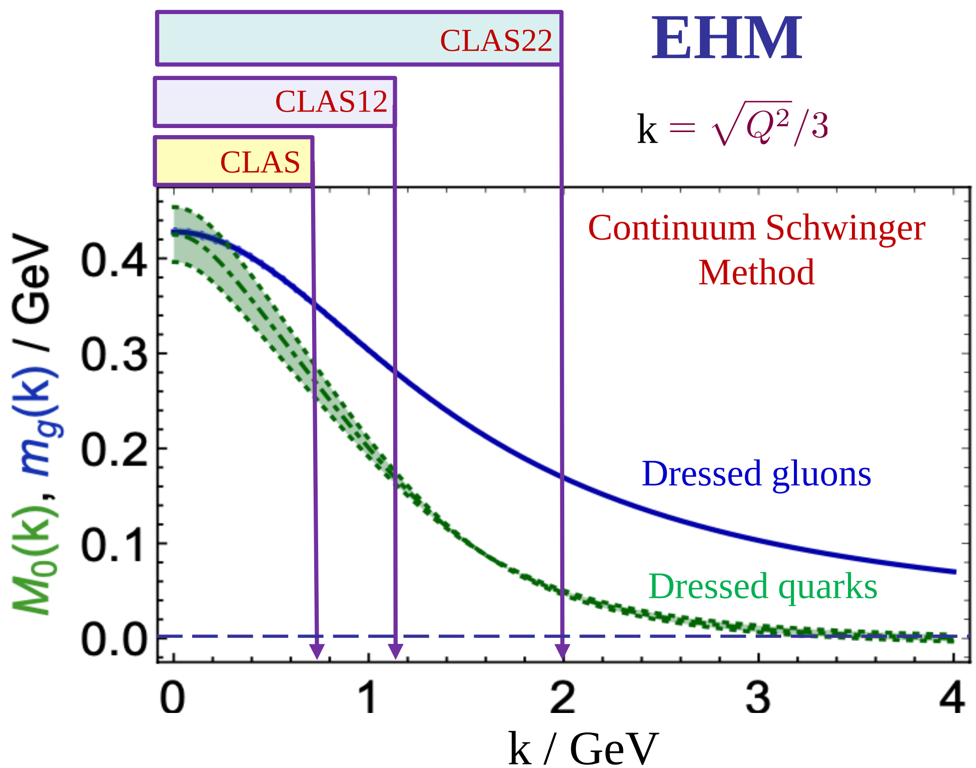


Both EIC and EIcC would need much higher luminosity to carry out this program.

Luminosity “frontier” is the *unique* advantage of JLab.

# Hadron Structure Needs for CLAS22

- Beam energy 22 GeV
- Nearly 4π acceptance

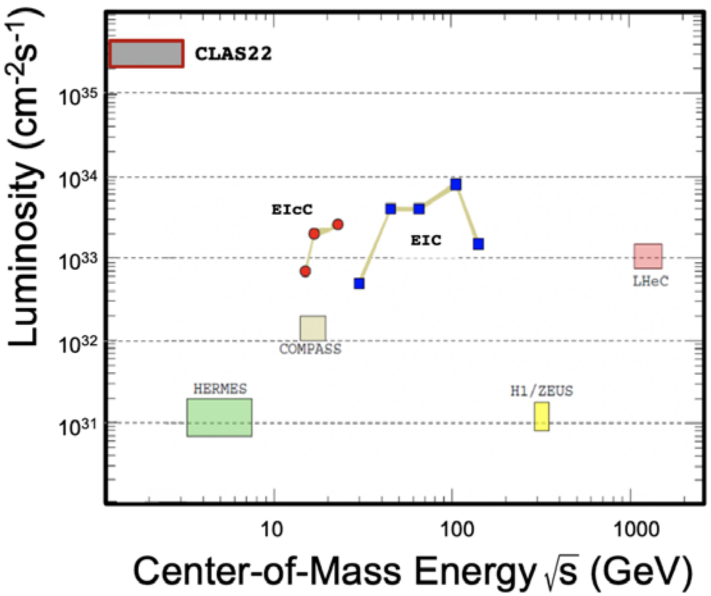


Both EIC and EIcC would need much higher luminosity to carry out this program.

- High luminosity detector
- High momentum resolution
- Studies of exclusive reactions

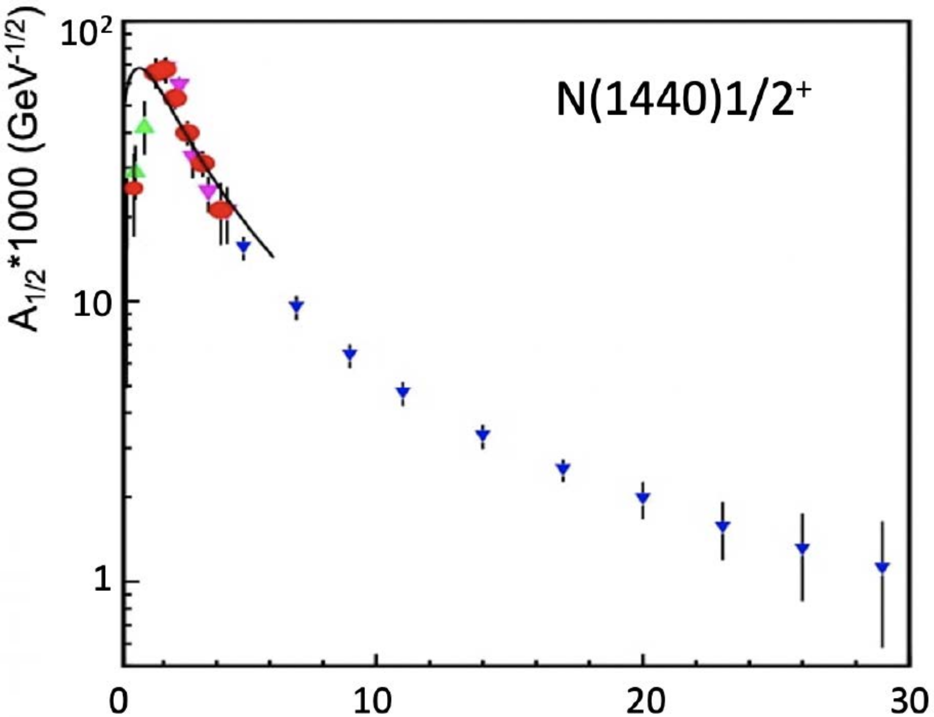


Extend up to 30+ $GeV^2$

Luminosity “frontier” is the *unique* advantage of JLab.

# JLab @ 22 GeV and EHM

e-Print: 2306.09360
accepted in EPJA

Strong Interaction Physics at the Luminosity Frontier
with 22 GeV Electrons at Jefferson Lab

### 6.5 Bound Three-Quark Structure of Excited Nucleons and Emergence of Hadron Mass

D.S. Carman, R.W. Gothe, V.I. Mokeev, C.D. Roberts

#### 6.5.1 The Emergent Hadron Mass Paradigm



The Standard Model of Particle Physics has one well-known mass-generating mechanism for the most elementary constituents of Nature, *viz.* the Higgs boson [295, 296], which is critical to the evolution of the Universe. Yet, alone, the Higgs is responsible for just 1% of the visible mass in the Universe. Visible matter is constituted from nuclei found on Earth and the mass of each such nucleus is largely the sum of the masses of the nucleons they contain. However, only 9 MeV of a nucleon's mass, $m_N = 940$ MeV, is directly generated by Higgs boson couplings into quantum chromodynamics (QCD). Evidently, as highlighted by Fig. 46, Nature has another, very effective, mass-generating mechanism. Often called emergent hadron mass (EHM) [202, 297–299], it is responsible for 94% of $m_N$, with the remaining 5% generated by constructive interference between EHM and the Higgs boson. This makes studies of the structure of ground and excited nucleon states in experiments with electromagnetic probes a most promising avenue to gain insight into the strong interaction dynamics that underlie the emergence of the dominant part of the visible mass in the Universe [105, 202, 300–302].

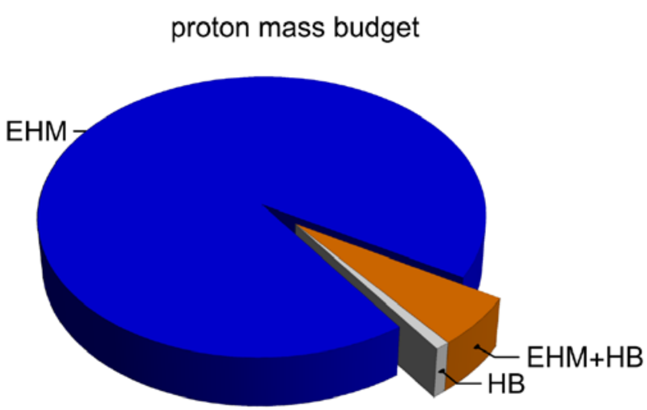


Figure 46: Proton mass budget, drawn using a Poincaré-invariant decomposition: emergent hadron mass (EHM) = 94%; Higgs boson (HB) contribution = 1%; and EHM+HB interference = 5%. (Separation at renormalization scale $\zeta = 2$ GeV, calculated using information from Refs. [22, 303–305]).

…

* 16 editors
444 authors

# $\gamma_v pN^*$ and EHM

particles

MDPI

e-Print: 2301.07777
Particles 6 (2023) 1, 416-439

Review

*Preprint no.* JLAB-PHY-23-3744, NJU-INP 069/23

## Nucleon Resonance Electroexcitation Amplitudes and Emergent Hadron Mass

Daniel S. Carman [1,†], Ralf W. Gothe [2,†], Victor I. Mokeev [1,†], and Craig D. Roberts [3,4,†,*]

**Abstract:** Understanding the strong interaction dynamics that govern the emergence of hadron mass (EHM) represents a challenging open problem in the Standard Model. In this paper we describe new opportunities for gaining insight into EHM from results on nucleon resonance ($N^*$) electroexcitation amplitudes (*i.e.* $\gamma_v pN^*$ electrocouplings) in the mass range up to 1.8 GeV for virtual photon four-momentum squared (*i.e.* photon virtualities $Q^2$) up to 7.5 GeV$^2$ available from exclusive meson electroproduction data acquired during the 6-GeV era of experiments at Jefferson Laboratory (JLab). These results, combined with achievements in the use of continuum Schwinger function methods (CSMs), offer new opportunities for charting the momentum dependence of the dressed quark mass from results on the $Q^2$-evolution of the $\gamma_v pN^*$ electrocouplings. This mass function is one of the three pillars of EHM and its behavior expresses influences of the other two, *viz*. the running gluon mass and momentum-dependent effective charge. A successful description of the $\Delta(1232)3/2^+$ and $N(1440)1/2^+$ electrocouplings has been achieved using CSMs with, in both cases, common momentum-dependent mass functions for the dressed quarks, for the gluons, and the same momentum-dependent strong coupling. The properties of these functions have been inferred from nonperturbative studies of QCD and confirmed, *e.g.*, in the description of nucleon and pion elastic electromagnetic form factors. Parameter-free CSM predictions for the electrocouplings of the $\Delta(1600)3/2^+$ became available in 2019. The experimental results obtained in the first half of 2022 have confirmed the CSM predictions. We also discuss prospects for these studies during the 12-GeV era at JLab using the CLAS12 detector, with experiments that are currently in progress, and canvass the physics motivation for continued studies in this area with a possible increase of the JLab electron beam energy up to 22 GeV. Such an upgrade would finally enable mapping of the dressed quark mass over the full range of distances (*i.e.* quark momenta) where the dominant part of hadron mass and $N^*$ structure emerge in the transition from the strongly coupled to perturbative QCD regimes.

check for updates

**Citation:** Carman, D.S.; Gothe, R.W.; Mokeev, V.I.; and Roberts, C.D. Nucleon Resonance Electroexcitation and Emergent Hadron Mass. *Particles* **2023**, *1*, 1–23. https://doi.org/

Received: 2023 Jan 09
Accepted:
Published: